Mobilome-driven segregation of the resistome in biological wastewater treatment

Laura de Nies[1], Susheel Bhanu Busi[1], Benoit Josef Kunath[1], Patrick May[2] and Paul Wilmes[1,3,#]

[1]Systems Ecology Group, Luxembourg Centre for Systems Biomedicine, University of Luxembourg, Esch-sur-Alzette, Luxembourg

[2]Bioinformatics Core, Luxembourg Centre for Systems Biomedicine, University of Luxembourg, Esch-sur-Alzette, Luxembourg

[3]Department of Life Sciences and Medicine, Faculty of Science, Technology and Medicine, University of Luxembourg, Esch-sur-Alzette, Luxembourg.

[#]Corresponding author: Paul Wilmes; paul.wilmes@uni.lu

Abstract

Biological wastewater treatment plants (BWWTP) are considered to be hotspots of evolution and subsequent spread of antimicrobial resistance (AMR). Mobile genetic elements (MGEs) promote the mobilization and dissemination of antimicrobial resistance genes (ARGs) and are thereby critical mediators of AMR within the BWWTP microbial community. At present, it is unclear whether specific AMR categories are differentially disseminated via bacteriophages (phages) or plasmids. To understand the segregation of AMR in relation to MGEs, we analyzed meta-omic (metagenomic, metatranscriptomic and metaproteomic) data systematically collected over 1.5 years from a BWWTP. Our results showed a core group of fifteen AMR categories which were found across all timepoints. Some of these AMR categories were disseminated exclusively (bacitracin) or primarily (aminoglycoside, MLS and sulfonamide) via plasmids or phages (fosfomycin and peptide), whereas others were disseminated equally by both MGEs. Combined and timepoint-specific analyses of gene, transcript and protein abundances further demonstrated that aminoglycoside, bacitracin and sulfonamide resistance genes were expressed more by plasmids, in contrast to fosfomycin and peptide AMR expression by phages, thereby validating our genomic findings. In the analyzed communities, the dominant taxon *Candidatus* Microthrix parvicella was a major contributor to several AMR categories whereby its plasmids primarily mediated aminoglycoside resistance. Importantly, we also found AMR associated with ESKAPEE pathogens within the BWWTP, for which MGEs also contributed differentially to the dissemination of ARGs. Collectively our findings pave the way towards understanding the segmentation of AMR within MGEs, thereby shedding new light on resistome populations and their mediators, essential elements that are of immediate relevance to human health.

Introduction

Throughout human history, bacterial infections have been a major cause of both disease and mortality (Bonilla and Muniz, 2009). The discovery as well as the subsequent development and medical use of antibiotics have provided effective

2

44 treatment options which limited the development and spread of bacterial pathogens.

45 However, the use of antibiotics has exacerbated the emergence of antimicrobial

46 resistance (AMR) in both commensal and pathogenic bacteria (Wright, 2007). As a

47 result, AMR, as the "silent pandemic", has become a prevalent threat to human health

48 (Brogan and Mossialos, 2016; Mahoney et al., 2021; O'Neill, 2014).

49   From a public health perspective, biological wastewater treatment plants

50 (BWWTPs) are considered hotspots of AMR due to the convergence of antibiotics with

51 resistant, potentially pathogenic microorganisms originating from both the general

52 population as well as agriculture and healthcare services (Alexander et al., 2020a;

53 Rodríguez-Molina et al., 2019). Additionally, the mobilization of antimicrobial resistance

54 genes (ARGs) through rampant horizontal gene transfer (HGT) promotes the

55 dissemination of AMR within the BWWTP microbial community (von Wintersdorff et al.,

56 2016). Therefore, BWWTPs represent an environment exceptionally suited for the

57 evolution and subsequent spread of AMR (Calero-Cáceres et al., 2014; Chen et al.,

58 2013). To date, more than 32 studies have documented the role of BWWTPs as key

59 reservoirs of AMR (Fouz et al., 2020). Furthermore, BWWTPs generally do not contain

60 the necessary infrastructure to remove either ARGs or resistant bacteria, which are

61 released into the receiving water via the effluent, promoting its spread in the

62 environment at large (Alexander et al., 2020b). Most often these are surface water

63 bodies such as rivers, which contribute to the further dissemination of AMR and

64 resistant bacteria among environmental microorganisms (Singer et al., 2016). Acquired

65 resistance may in turn be carried over to humans and animals using these water

66 resources. In fact, there is strong evidence suggesting that ARGs from environmental

67 bacteria can be taken up by human-associated and pathogenic bacteria (Nadeem et al.,

68 2020; Trinh et al., 2018). From an epidemiological and surveillance perspective,

69 BWWTPs also provide samples representative of entire populations (Hendriksen et al.,

70 2019). As such, BWWTPs have recently been crucial for the monitoring of SARS-CoV-2

71 within the human population (Herold et al., 2021). Overall, to increase our

72 understanding of the dissemination of AMR and the underlying mechanisms as well as

73 its general prevalence, it is necessary to map the resistome of various environments

74 starting with biological BWWTPs because it is critical to unravel the extent to which they

75 act as reservoirs for the dissemination of antimicrobial resistance genes (ARGs) to
76 bacterial pathogens. Moreover, understanding the community-level overviews of the
77 ARG potential and its expression, coupled with population-level linking, including to
78 pathogens, may allow for efficient monitoring of pathogenic and AMR potential with
79 broad impacts on human health.

80   The presence of resistance genes and mobile genetic elements (MGEs) along
81 with sub-inhibitory antibiotic selection pressures may facilitate HGT of ARGs into new
82 hosts through the mobilome (von Wintersdorff et al., 2016). Previous work has in
83 particular shown that antibiotic selection pressures may alter HGT processes, thereby
84 increasing the number of resistance elements which reside on mobile DNA (Datta and
85 Hughes, 1983). Acquisition of ARGs via MGEs primarily occurs through two
86 mechanisms: conjugation or transduction (MacLean and San Millan, 2019). In
87 conjugation, plasmids carrying one or more resistance genes are transferred between
88 microorganisms (Carattoli, 2013), while in transduction bacteriophages carrying ARGs
89 infect bacteria and integrate their genome into those of the host thereby conferring
90 resistance (Chiang et al., 2019). Of these mechanisms, conjugation is often thought to
91 have the greatest influence on the dissemination of ARGs, while transduction is deemed
92 less important (von Wintersdorff et al., 2016). In general terms, studies concerning AMR
93 and its dissemination focus either on phage (Lood et al., 2017; Strange et al., 2021) or
94 plasmids solely (Li et al., 2019). Alternatively, the two are treated collectively (Alexander
95 et al., 2020b; Che et al., 2019) without a comprehensive comparative analysis. This
96 circumstance has created a knowledge gap whereby the contributions of plasmids and
97 phages as independent entities to AMR transmission within complex communities, such
98 as those found in biological BWWTPs, is largely unknown.

99   To shed light on the dissemination and potential segregation of AMR within
100 MGEs in a WTTP microbial community, we leveraged longitudinal meta-omics data
101 (metagenomics, metatranscriptomics and metaproteomics). Samples collected for 51
102 consecutive weeks over a period of 1.5 years were used to characterize the resistome.
103 We found that several bacterial orders such as Acidimicrobiales, Burkholderiales and
104 Pseudomonadales were associated with 29 AMR categories across all timepoints. Our
105 longitudinal analysis suggests that MGEs are important drivers of AMR dissemination

4

106   within BWWTPs. More importantly, we reveal that MGEs, i.e. plasmidomes and
107   phageomes, contribute differentially to AMR dissemination. Furthermore, we observed
108   this phenomenon in clinically-relevant taxa such as the ESKAPEE pathogens (Reza et
109   al., 2019), for which plasmids and phages were exclusively associated with specific
110   ARGs. Collectively, our data suggest that BWWTPs are critical reservoirs of AMR which
111   show clear evidence for the segregation of distinct AMR genes within MGEs especially
112   in complex microbial communities. In general, we believe that these findings may
113   provide crucial insights into the segregation of the resistome via the mobilome in any
114   and all reservoirs of AMR, including but not limited to animals, humans, and other
115   environmental systems.

116   Results

117   Longitudinal assessment of the resistome within a BWWTP

118   To characterize the BWWTP resistome, we sampled a municipal BWWTP on a
119   weekly basis over a 1.5 year period (ranging from 21-03-2011 to 03-05-2012) (Herold et
120   al., 2020; Martínez Arbas et al., 2021). Metagenomic and metatranscriptomic reads
121   were preprocessed, and both sets of reads co-assembled using the Integrated Meta-
122   omic Pipeline as described previously (Narayanasamy et al., 2016). Subsequently,
123   utilizing the PathoFact pipeline (de Nies et al., 2021) on the assembled contigs
124   (*Methods*), we resolved the BWWTP resistome. This analysis revealed the presence of
125   29 different categories of AMR within the BWWTP. Subsequent longitudinal analyses
126   highlighted enrichments in aminoglycoside, beta-lactam and multidrug resistance genes
127   (Fig. 1a). Concomitantly, we observed specific shifts in the AMR profiles over time. For
128   example, a transient change at two timepoints (13-05-2011, 08-02-2012) highlighted a
129   steep increase in resistance genes corresponding to glycopeptide resistance. Other
130   AMR categories, such as diaminopyrimidine resistance, exhibited a less drastic but
131   more fluid change in longitudinal abundance observable over multiple timepoints.
132   Additionally, AMR categories were found to persist over time within the BWWTP
133   (Fig. 1b). A core group of 15 AMR categories in total were identified and found to be
134   present across the 1.5 year sampling period. These included aminoglycoside, beta-

lactam and multidrug resistance genes, which contributed the most to the pool of ARGs. A further six (aminocoumarin, aminoglycoside:aminocoumarin, elfamycin, nucleoside, triclosan and unclassified) AMR categories were found to be prevalent (>75% of all timepoints), while another three AMR categories were moderately (50 - 75% of all timepoints) present over time (Fig. 1b). Five other categories were rarely present within the BWWTP, with resistance corresponding to acridine dye only present at six of the timepoints. Altogether, this emphasized that the BWWTP resistome varies over time, substantiating the requirement for a longitudinal analysis to obtain an accurate overview of the community's overall resistome.

Although the data thus far provided a clear overview of the BWWTP from a metagenomic perspective, it did not provide any information regarding AMR expression. We therefore utilized the corresponding metatranscriptomic dataset to investigate the expression of identified ARGs and monitor their changes, within the BWWTP, over time. In contrast to the metagenomic data, we observed a difference in AMR expression levels for several categories. Aminoglycoside, beta-lactam, and multidrug resistance identified at high levels in metagenomic information were also highly expressed within the BWWTP (Fig. 1c). However, peptide resistance demonstrated the highest expression levels of all the AMR categories. We further investigated which ARG subtypes contributed to the identified peptide resistance category and found that ~90% of the expressed peptide resistance was directly contributed by a single resistance gene, *YojI*, which was found to be widely distributed among the major taxa comprising the BWWTP community such as the Comamonadaceae (Figure 1-figure supplement 1). YojI is typically associated with resistance to microcins by reducing the intracellular concentration of the toxic antibiotic peptide (Delgado et al., 2005). The high incidence of this gene indicates a broad adaptive strategy amongst the microbial populations in the BWWTP against these specific stressors.

Microbial community and co-occurrence patterns of AMR

Based on the previously identified microbial community (Herold et al., 2020), we hypothesized that the abundant and prevalent bacterial orders such as Acidimicrobiales were major contributors to the abundance in ARGs observable via metagenomics. To

165 further investigate the contribution to AMR by the distinct microbial populations, we

166 linked AMR genes to the contig-based taxonomic annotations of the assemblies

167 (Methods). Herein, we identified a wide variety of taxonomic orders contributing to AMR,

168 with multiple orders often contributing to the same resistance categories (Figure 2-figure

169 supplement 1). Overall, taxa belonging to Acidimicrobiales, followed by Burkholderiales,

170 were found to encode most of the ARGs (Fig. 2a). Additionally, the abundance of ARGs

171 linked to taxonomy varied over time. This was most noticeable during a five-week period

172 (autumn: 02-11-2011 to 29-11-2011), where a decrease in abundance in ARGs linked to

173 Acidimicrobiales and Bacteroidales was observed coinciding with an increase in ARG

174 abundance in Pseudomonadales and Lactobacillales.

175 Since the order Acidimicrobiales was found to be linked to the highest

176 abundance in ARGs, we further resolved the taxonomic affiliation and identified the

177 species *Candidatus* Microthrix parvicella (hereafter known as *M. parvicella*) to be the

178 main contributor to AMR. *M. parvicella* was previously found to dominate this microbial

179 community (Martínez Arbas et al., 2021) and is a well-characterized bacterium

180 commonly occurring in the BWWTP (Calusinska et al., 2018). Overall, aminoglycoside,

181 beta-lactam, multidrug and peptide resistance were found to be abundant in this species

182 (Fig. 2b), with aminoglycoside resistance demonstrating the highest expression levels

183 as confirmed through metatranscriptomic analysis (Figure 2-figure supplement 2).

184 Although it was not surprising to find a high abundance of ARGs linked to this species,

185 the longitudinal variation in the abundances of these ARGs was nevertheless surprising

186 (Fig. 2b). Furthermore, coupled to a decrease in the abundance of *M. parvicella* itself

187 (Martínez Arbas et al., 2021), we observed an almost complete decrease in ARGs at

188 two timepoints (23-11-2011 and 29-11-2011). However, the *M. parvicella* population

189 recovered to levels resembling the earlier timepoints in conjunction with the abundances

190 in ARGs towards the end of the sampling period (Fig. 2a, Fig. 2b), underlining their

191 overall contribution to AMR within this BWWTP. Alternatively, it is plausible that the

192 dominance of *M. parvicella* is attributable to the encoded ARGs, which in turn, may

193 confer a fitness advantage.

194 In order to determine whether the abundances in ARGs may be directly

195 associated with the community composition over time, co-occurrence patterns between

7

196   ARG subtypes and taxa (genus level) were explored using the metagenomic data.
197   Bipartite network analyses (Fig. 2c) demonstrated that ARGs, within or across ARG
198   types and microbial taxa, showed clear and distinct co-occurrence patterns within the
199   BWWTP. These patterns indicated a strong segregation of distinct, taxa-specific ARG
200   subtypes within the BWWTP community over time. One clear example was that of *M.*
201   *parvicella* which encoded different aminoglycoside resistance genes (Fig. 2c). Thus, the
202   abundance of this bacterium along with the aminoglycoside ARGs were highly
203   correlated.

204   Monitoring pathogenic microorganisms within BWWTPs

205   In conjunction with the families observed within BWWTPs, we also found that
206   certain ESKAPEE pathogens (Reza et al., 2019), such as *Klebsiella* spp. and
207   *Pseudomonas* spp., demonstrated co-occurring patterns with ARGs (Fig. 2c).

208   As previously mentioned, BWWTPs represent a collection of potentially
209   pathogenic microorganisms originating from, among others, the human population.
210   Moreover, evidence suggests that ARGs from environmental and commensal bacteria
211   can spread to pathogenic bacteria through HGT (MacLean and San Millan, 2019).
212   Therefore, we assessed the presence of AMR in the extended priority list of pathogens
213   (Table 1), characterized as such by the WHO (Tacconelli et al., 2018), using both
214   metagenomics and metatranscriptomics.

215

216   Table 1: WHO priority list for research and development of new antibiotics for
217   antibiotics-resistant bacteria (Tacconelli et al., 2018).

Bacteria	Priority	Organism detected	Resistance detected
Acinetobacter baumannii	Critical	+	+
Pseudomonas aeruginosa	Critical	+	+
Enterobacteriaceae	Critical	+	+
Enterococcus faecium	high	+	+
Staphylococcus aureus	high	+	+
Helicobacter pylori	high	+	+

Campylobacter spp	high	+	-
Salmonella spp	high	+	+
Neisseria gonorrhoeae	high	+	-
Streptococcus pneumoniae	medium	+	+
Haemophilus influenzae	medium	+	-
Shigella spp	medium	+	+

218

219   Of the identified pathogens (Table 1), we found that *Pseudomonas aeruginosa*,
220   both encoded and expressed the highest abundance of ARGs, followed by
221   *Acinetobacter baumannii*, over time within the BWWTP (Fig. 3). Moreover, an increase
222   in ARG abundance and expression was observed in *Pseudomonas aeruginosa* during
223   the time period, during which the otherwise dominant *M. parvicella* demonstrated
224   reduced abundance (Fig. 2b & Fig. 3).

225   Differential transmission of antimicrobial resistance via mobile genetic
226   elements

227   As previously described (Beceiro et al., 2013; Wee et al., 2020), the mobilome is
228   a major contributor to the dissemination of AMR within a microbial community.
229   Consequently, to understand (i) the role of MGE-mediated AMR transfer within the
230   BWWTP, and (ii) to identify differential contribution of the mobilome to the dissemination
231   of AMR, we identified both plasmids and phages within the metagenome and linked
232   these to the respective ARGs. While, as expected, the majority of ARGs was found to
233   be encoded on the bacterial chromosome (Figure 4-figure supplement 1), we also found
234   that plasmids contributed to an average of 10.8% of all ARGs, while phage contributed
235   to an average of 6.8% of all resistance genes, in agreement with the general hypothesis
236   that conjugation has the greatest influence on the dissemination of ARGs (*adj.p* < 0.05,
237   One-way ANOVA) (MacLean and San Millan, 2019). This phenomenon, however,
238   varied across time within the BWWTP (Fig. 4a).

239   When investigating the dissemination of AMR via MGEs, most reports typically
240   focus on either phages or plasmids individually, or both as collective contributors to

241 transmission (Slizovskiy et al., 2020). To date and to our knowledge, the respective
242 contributions of phage and plasmid to AMR transmission have not been subjected to a
243 comprehensive comparative analysis. To facilitate a systematic, comparative view of
244 MGE-mediated AMR, we assessed the segregation of MGEs with respect to AMR and
245 found that phages and plasmids contributed differentially to AMR (Figure 4-figure
246 supplement 2). Specifically, we tested 28 AMR categories with respect to their
247 association with MGEs and found a significant difference in six AMR categories when
248 comparing ARGs encoded by phages and plasmids ($adj.p$ < 0.05, Two-way
249 ANOVA)(Fig. 4b). Aminoglycoside, bacitracin, MLS (i.e. macrolide, lincosamide and
250 streptogramin) and sulfonamide resistance were found to be primarily encoded by
251 plasmids, whereas fosfomycin and peptide resistance were found to be associated with
252 phages.

253   To further understand AMR in relation to the community dynamics, we
254 investigated the abundance and segregation of the above-mentioned significant
255 resistance categories at different timepoints within the BWWTP. We observed ARG
256 abundances varied over time both in phages (Fig. 4c) as well as plasmids (Fig. 4d). For
257 instance, the abundance in aminoglycoside and sulfonamide resistance, which was
258 encoded primarily by plasmids (Figure 5-figure supplement 1a), fluctuated widely over
259 time in both phages and plasmids (Fig. 4c). Additionally, plasmid-mediated sulfonamide
260 resistance was reduced at 23-11-2011, followed by its highest abundance a week later
261 (29-11-2011), while subsequently again decreasing. Similarly, in line with the above
262 observations, fosfomycin and peptide resistance genes, while segregating within
263 phages, demonstrated significant fluctuations over time (Fig. 4d). In addition to the
264 metagenome, we also contextualized the localization of the expressed ARGs within
265 MGEs based on the metatranscriptomic information. Specifically, we found that
266 plasmids demonstrated a significantly increased expression of aminoglycoside along
267 with bacitracin and sulfonamide resistance genes, while the expression of glycopeptide,
268 mupirocin and peptide resistance genes were primarily enriched in phages (Fig. 5a).
269 These observations pertaining to plasmid-mediated AMR were in line with the
270 metagenomic findings (Fig. 4b). Only peptide resistance was observed to be expressed

271 via phages in contrast to the differential enrichment of fosfomycin resistance observable

272 in the metagenomic data.

273 ## Taxonomic affiliations of MGE-derived resistance genes

274   When assessing the differential contributions of MGEs to AMR, we found

275 congruency between plasmids and phages to the AMR categories and taxonomic

276 affiliations (Fig. 5b). For example, in the metagenomic data MGEs (phage and plasmid)

277 were predominantly associated with the same AMR category and subsequently the

278 same taxa. However, some exceptions were observed with specific taxa associated with

279 AMR either through plasmids or phages. For instance, MLS resistance in Bacteroidales

280 and Nostocales was mediated solely through plasmids, whereas the same resistance

281 category was mediated by phage in Bifidobacteriales, indicating segregation of AMR

282 between taxa and MGEs.

283   As most bacteria harbor MGEs, we queried whether the MGE-mediated AMR

284 categories were linked to the abundance of some of the earlier reported taxa.

285 Interestingly, we found that peptide resistance encoded by *M. parvicella* was solely

286 associated with phages, while aminoglycoside resistance was primarily correlated with

287 plasmids (Figure 5-figure supplement 1b). Other highly abundant taxa such as

288 *Pseudomonas* and *Comamonas* (Figure 5-figure supplement 1c-d), on the other hand,

289 were correlated with sulfonamide resistance in addition to aminoglycoside resistance

290 encoded on plasmids (Fig. 5b). This was further reflected within the metatranscriptome

291 data where in taxa such as Acidimicrobiales the expression levels of aminoglycoside

292 resistance were solely associated with plasmids (Figure 5-figure supplement 2a).

293 Additionally, in the Burkholderiales family, peptide resistance was found to be

294 expressed through phages (Figure 5-figure supplement 2b).

295   We also found a clear segregation of the mobilome with respect to individual

296 pathogens in the metagenome. Interestingly, plasmids were exclusively associated with

297 AMR in six out of the fourteen relevant taxa (Fig. 5c). These included *Streptococcus*

298 *pneumoniae, Staphylococcus aureus, Shigella flexneri, Klebsiella pneumoniae,*

299 *Enterobacter kobei* and *Enterobacter hormaechei*. Furthermore, the plasmids were also

300 associated with conferring peptide, multidrug, MLS, beta-lactam, fluoroquinolone,

301   bacitracin, aminoglycoside, aminoglycoside:aminocumarin and sulfonamide resistance.

302   Phages were exclusively associated with glycopeptide and aminoglycoside resistance *in*

303   *Salmonella enterica*. Overall, our results revealed for the first time the key segregation

304   patterns of AMR via the mobilome in taxa that are of relevance to human health and

305   disease. Moreover, substantiating the metagenomic data, the pathogenic bacteria *S.*

306   *pneumoniae*, *S. aureus*, *K. pneumoniae*, *E. kobei* and *E. hormaeche* were found to

307   express ARGs solely associated with plasmids (Fig. 5c). Collectively, these findings

308   indicate an imminent threat to global health due to the potential dissemination of

309   resistant pathogens across reservoirs.

Metaproteomic validation of AMR abundance and expression

311   In order to expand our findings with the expression (metatranscriptomic)

312   analyses on the BWWTP, we further used the corresponding metaproteomic data to

313   offer complementary information at the protein level. Similar to the metagenome data

314   we found protein expression linked to aminoglycoside, beta-lactam and multidrug

315   resistance, over time within the BWWTP (Figure 6-figure supplement 1). Proteins,

316   especially those linked to multidrug resistance were found to increase over time.

317   To further unravel AMR expression and assess its stability across time, we

318   estimated the normalized protein index (NPI) per gene, as discussed in the Methods, by

319   integrating all of the multi-omic data. The estimated NPI demonstrated stable levels of

320   aminoglycoside and multidrug resistance within the BWWTP (Fig. 6a). Specifically,

321   proteins conferring multidrug resistance were found to increase over time, which is in

322   line with the gene- and expression-level observations. Furthermore, we contextualized

323   the normalized proteins conferring AMR to their localization on MGEs. We identified five

324   resistance categories, i.e. aminoglycoside, beta-lactam, sulfonamide, multidrug and

325   tetracycline resistance, to be expressed through MGEs (Fig. 6b). Of these categories

326   we found that aminoglycoside resistance, in concordance with the gene and expression

327   levels, was more strongly associated with plasmids than phages (*adj.p* < 0.05, Two-way

328   ANOVA). We further found that the MGE-mediated AMR categories were associated

329   with specific microbial taxa. with plasmid-mediated aminoglycoside resistance found to

330   be strongly associated with the previously mentioned *M. parvicella* (Fig. 6b). On the

331 other hand, we did not identify any peptides associated with the ESKAPEE pathogens
332 via metaproteomics.

Discussion

334   The surveillance of wastewaters for the identification of microbial molecular
335 factors is a critical tool for identifying potential pathogens. This has been highlighted
336 recently with the tracking of SARS-CoV-2 within wastewater treatment plants to assess
337 viral prevalence and load within a given community (Westhaus et al., 2021). Such
338 approaches have also been employed for screening for antimicrobial resistance at a
339 population level (Kwak et al., 2015; Reinthaler et al., 2013). So far, several studies
340 (Calero-Cáceres et al., 2014; Hendriksen et al., 2019; Parsley et al., 2010;
341 Szczepanowski et al., 2009) have characterized the proliferation of ARGs and antibiotic
342 resistant bacteria in BWWTP. Szczepanowski *et al.* (Szczepanowski et al., 2009)
343 identified 140 clinically relevant plasmid-derived ARGs in a BWWTP metagenome while
344 Parsley *et al.* (Parsley et al., 2010) characterized ARGs from bacterial chromosomes,
345 plasmids and in viral metagenomes found in a BWWTP. Further studies have shown
346 that conventional BWWTP processes at best only partially remove ARGs from the
347 effluent and may find their way into the urban water cycle (Hiller et al., 2019; Proia et al.,
348 2018; Rodriguez-Mozaz et al., 2015). Wastewater treatment plants, therefore, are
349 crucial reservoirs of AMR, whose monitoring may allow for early-detection of AMR
350 within the human population feeding into the system. Here, we leveraged a systematic
351 and longitudinal sampling scheme from a BWWTP to identify diverse AMR categories
352 prevalent within the BWWTP microbial community. In line with the studies by
353 Szczepanowski *et al.* (Szczepanowski et al., 2009) and Parsley et al. (Parsley et al.,
354 2010), we found up to 29 AMR categories with several ARGs within the BWWTP. More
355 importantly, and unlike the previous studies, we linked the identified ARGs to clinically-
356 relevant ESKAPEE pathogens, which represent a growing global threat to human
357 health.

358   In our BWWTP samples, we identified a core group of 15 AMR categories that
359 were ubiquitous at all timepoints. In line with the above-mentioned reports, the observed
360 core resistance categories may reflect their abundance in the surrounding human

361   population (Aarestrup and Woolhouse, 2020). This has previously been reported by
362   Pärnänen *et al.* (Pärnänen *et al.*, 2019), Su *et al. (Su et al., 2017)* and Hendriksen *et al.*
363   (Hendriksen et al., 2019) where they showed that BWWTP AMR profiles correlate with
364   clinical antibiotic usage as well as other socio-economic and environmental factors.
365   Furthermore, bacteria are known to have innate defense mechanisms against inhibitory
366   secondary metabolites from other taxa (Frost et al., 2018). Therefore, one must be
367   cognizant of the phenomenon that the observed core group of AMR categories may
368   also be a proxy for the abundance of specific resistant bacteria. Despite this
369   observation, it is plausible that both anthropogenic and microbial sources for AMR play
370   a role in the observed resistance categories within the BWWTP. For instance, we found
371   that several AMR categories, including ancillary (prevalent, moderate, and rare) groups,
372   were associated with *M. parvicella* within the BWWTP. While the mechanisms
373   underlying the abundance of this taxon are numerous, the increased abundance of
374   ARGs are likely to contribute to its fitness advantage in this metal- and antibiotic-rich
375   environment (Baquero et al., 2008). Additionally, similar to the findings by Munck *et al.*
376   (Munck et al., 2015), we found a wide range of bacteria associated with AMR categories
377   including Acidimicrobiales, Burkholderiales and Rhodocyclales. On the other hand, we
378   report that taxa, including ESKAPEE pathogens, belonging to 25 bacterial orders were
379   associated with 29 AMR categories, compared to the eight bacterial orders reported
380   previously.

381   It is important to note that the mobilome plays a critical role in the dissemination
382   of AMR within microbial communities. AMR from resistant bacteria within the BWWTP
383   can quickly disseminate within the BWWTP (Che et al., 2019; Fouz et al., 2020),
384   including transmission from pathogenic to commensal species (Blake et al., 2003;
385   Brinkac et al., 2017). As a result, mediated through HGT, the BWWTP becomes a
386   hotspot for resistant bacteria, which are then released back into the receiving
387   environment (Turolla et al., 2018), and eventually the human population (Fouz et al.,
388   2020; Newton and McClary, 2019). Therefore, to limit the dissemination of AMR, it is
389   important to understand the role of MGEs within the BWWTP. Our comprehensive
390   analyses identified the differential contributions of AMR transmission mediated via
391   phage and plasmid (Fig. 7). Specifically, we identified clear segregation of

392 aminoglycoside, bacitracin, MLS and sulfonamide resistance categories with plasmids,
393 while fosfomycin and peptide resistance were increasingly encoded and conferred via
394 phages. While the association between these AMR categories and plasmids (Dubnau et
395 al., 1981; Galimand et al., 2003; Han et al., 2015; Razavi et al., 2017) or phages
396 (Torres-Barceló, 2018) are in line with previously reported results, differential analysis
397 between MGEs has not been previously reported and has not been performed on multi-
398 omic levels. In this study we report for the first time the systematic and extensive
399 comparison of AMR encoded and expressed by phages versus plasmids. Our results
400 indicating the segregation of ARGs within the ESKAPEE taxa via the MGEs further
401 provide insights into potential modes of AMR transmission among pathogens. Though
402 one cannot exclude the possibility of transmission of the above-mentioned ARGs via
403 other MGEs, identifying potential segregation of MGEs in the transmission of ARGs
404 brings us one step closer to identifying specific transmission paths and limiting the
405 spread of AMR. For example, some studies have reported plasmid "curing", the process
406 by which plasmids are removed from bacterial populations, as a strategy against
407 dissemination of AMR (Bouanchaud and Chabbert, 1971; Vrancianu et al., 2020). As
408 described by Buckner *et al.* (Buckner et al., 2018) plasmid curing, as well as other anti-
409 plasmid strategies, could both reduce AMR prevalence, and (re-)sensitize bacteria to
410 antibiotics (Buckner et al., 2018).

411   Although several methods and tools exist for the identification of MGEs, the
412 linkage to their respective bacterial hosts still remains a challenge. Our method
413 presented here involves taxonomic annotations of reconstructed genomic information as
414 a mean of linking bacteria to their corresponding MGEs using stringent
415 filtering/identification criteria. An alternative approach may involve targeted sequencing
416 of plasmids of interest and their respective hosts using the methodology established by
417 Li *et al.* (Li et al., 2018). However, to use such targeted sequencing approaches one
418 requires *a priori* information on which plasmids to focus on in contrast to our method
419 which is agnostic to such prior information. Furthermore, Hi-C-based methods
420 (Lieberman-Aiden et al., 2009; Maximilian O. Press et al., 2017) capture inter-
421 chromosomal junctions, such as plasmid-genome interactions. However, compared to
422 metagenomic approaches, these methods require different and extensive processing of

15

423   the samples prior to sequencing to induce covalent linkages among DNA molecules
424   (Lieberman-Aiden et al., 2009; Maximilian O. Press et al., 2017), therefore precluding
425   the use of this method for large-scale characterization efforts. Combining these
426   strategies in future studies with AMR categorization according to taxonomic affiliation as
427   well as linkage to specific MGEs will provide novel strategies for characterizing and
428   subsequently affecting MGE-mediated AMR.

429   By complementing the metagenomic analyses, metatranscriptomics conferred
430   essential information regarding gene expression within the resistome. For instance,
431   when comparing AMR expression levels of aminoglycoside, bacitracin, and sulfonamide
432   mediated via MGEs, it is noticeable that expression levels in plasmids mirror the
433   genomic content, i.e. they exhibited higher levels of expression when compared to
434   phage. On the other hand, glycopeptide and mupirocin resistance genes which were
435   highly expressed in phages were not reflected within the metagenomic data.
436   Additionally, we found the *YojI* resistance gene to be more highly expressed than any
437   other ARGs. To facilitate resistance against the peptide antibiotic microcin J25, the
438   outer membrane protein, TolC, in combination with *YojI* is required to export the
439   antibiotic out of the cell (Delgado et al., 2005). Microcin J25 belongs to the group of
440   ribosomally synthesized and post-translationally modified peptides (RiPPs) and has
441   antimicrobial activity against pathogenic genera such as *Salmonella* spp. and *Shigella*
442   spp. (Naimi et al., 2018). Interestingly, it has only recently been proposed as a
443   treatment option against *Salmonella enterica and* has been discussed in recent years
444   as a potential novel antibiotic (Ben Said et al., 2020). Based on these results, by
445   considering that BWWTPs may reflect both the presence of AMR within the human
446   population as well as be a hotspot of dissemination and generation of new AMR,
447   surveillance of BWWTPs must be emphasized when developing new antibiotics. Our
448   findings collectively suggest that the differential capacity of MGEs to disseminate AMR,
449   coupled with longitudinal and expression-level analyses are crucial for monitoring
450   human health conditions. More importantly, we report for the first time that BWWTP
451   monitoring for AMR may allow for early detection of resistance mechanisms previously
452   undescribed in BWWTP.

453   Finally, we applied an integrated multi-omic approach to improve our knowledge
454   on the functional potential of AMR and simultaneously validate the abundance and
455   expression findings of the ARGs. By normalizing the metaproteomic results with the
456   normalized expression of genes we were able to assess the stability of expressed AMR
457   across time. We find that our methodology allows for an unbiased assessment of overall
458   expression accounting for gene copy abundance and expression. These findings
459   support the notion that the AMR genes may serve as sentinels or indicators of the
460   presence of particular antimicrobial agents. However, it is plausible that we are only
461   identifying the most abundant proteins and/or proteins that are more stable over time,
462   and do not capture the entirety of the proteome profiles. Factors such as protein decay
463   rates (Cameron and Collins, 2014) among others, may additionally influence this
464   assessment. Irrespective of these observations, we identified segregation of AMR
465   categories with respect to plasmids and phages.

466   Our findings also highlighted the potential for identifying segregation of AMR via
467   specific MGEs with an aim towards possible therapeutic and mitigation strategies via for
468   example plasmid curing. Furthermore, we demonstrate that longitudinal analyses are
469   required to survey AMR within BWWTPs due to the variations in the resistome across
470   time. These shifts may either be representative of a shift within the human population
471   itself, which in turn could be associated with the concurrent use of antibiotics at a given
472   time, or competition within the microbial community. In any case, an independent or
473   static analysis of the various time points may show an incomplete view of the BWWTP
474   resistome, thus underlining the importance of our longitudinal resistome analyses.
475   Overall, our findings suggest that BWWTPs are critical reservoirs of AMR, potentially
476   allowing for early detection and monitoring of pathogens. In addition, BWWTP
477   monitoring may allow detection of resistance mechanisms linked to the introduction of
478   new antimicrobials. Finally, BWWTPs may serve as a model for understanding the
479   segregation of MGEs through AMR.

Methods

Sampling and biomolecular extraction

From within the anoxic tank of the Schifflange municipal biological wastewater treatment plant (located in Esch-sur-Alzette, Luxembourg; 49° 30′ 48.29″ N; 6° 1′ 4.53″ E) individual floating sludge islets were sampled according to previous described protocols (Herold et al., 2020). Sampling was performed starting on 21-03-21 till 03-05-2012 in approximately one-week intervals resulting in a total of 51 samples. DNA, RNA and proteins were extracted from the samples in a sequential co-isolation procedure as previously described (Roume et al., 2013).

Sequencing and data processing for metagenomics and metatranscriptomics

Paired-end libraries were generated for metagenomics with the AMPure XP/Size Select Buffer Protocol following a size selection step recommended by the standard protocol. Libraries for metatranscriptomics were prepared from RNA after washing stored extractions with ethanol and depletion of rRNAs with the Ribo-Zero Meta-Bacteria rRNA Removal Kit (Epicenter). Subsequently, the ScriptSeq v2 RNA-seq library preparation kit (Epicenter) was used for cDNA library preparation, followed by sequencing on an Illumina Genome Analyses IIx instrument with 100-bps paired-end protocol. Processing and iterative co-assembly of metagenomic and metatranscriptomic reads was done using the Integrated Meta-omic Pipeline (Narayanasamy et al., 2016) (IMP v1.3; available at https://r3lab.uni.lu/web/imp/). For read processing, Illumina Truseq2 adapters were trimmed, and reads of human origin were filtered out, followed by a de novo assembly with MEGAHIT (Li et al., 2015) v1.0.6. For the assembly, both metagenomic and metatranscriptomic reads were co-assembled to increase contiguity of the assemblies and to improve read usage. Additional information regarding the read coverage and depth for each sample is available at https://git-r3lab.uni.lu/laura.denies/lao_scripts.

Identification of antimicrobial resistance genes, mobile genetic elements and taxonomy

The assembled contigs from IMP were used as input for PathoFact (de Nies et al., 2021), for the prediction of antimicrobial resistance genes and MGEs. ARGs were further collapsed into their respective AMR categories, as identified by PathoFact in accordance with those provided by the Comprehensive Antibiotic Resistance Database (CARD) (Alcock et al., 2020). Furthermore, utilizing PathoFact, AMR genes were linked to predicted MGEs (i.e. plasmids and phages) to track transmission of AMR. By considering all different predictions of MGEs, a final classification was made by PathoFact based on the genomic contexts of the AMR genes encoded on plasmids, phages or the organismal chromosomes, including the classification of those that could not be resolved (ambiguous). The AMR genes that could not be assigned to either the MGEs or bacterial chromosomes were subsequently referred to as unclassified genomic elements.

Identified ARGs and their categories were further linked to associated microbial taxonomies using the taxonomic classification system Kraken2 (Wood et al., 2019). Kraken2 was run on the contigs using the maxikraken2_1903_140GB (March 2019, 140GB) (https://lomanlab.github.io/mockcommunity/mc_databases.html) database (Wood et al., 2019). To ensure confidence in taxonomic classification, stringent cutoffs based on a minimum 70% identity of the contig with the database, across 90% of the contig length, was used (Wood et al., 2019). Since the same contig-based assembly file was used as input for PathoFact as well as for Kraken2, the prediction of antimicrobial resistance genes and mobile genetic elements as well as functional- and taxonomic-annotations were linked based on the contig they were encoded on (Fig. 8).

Though several methods and tools exist for the identification of plasmids and/or phages, tools identifying the respective bacterial hosts for MGEs are rare. The hosts for phages can be determined based on classification and linking of CRISPR and spacer sequences between bacterial and phage sequences respectively (Bland et al., 2007; Martínez Arbas et al., 2021). Plasmid hosts, on the other hand, due to the competence of plasmids (including self-replication, etc.), are difficult to identify (Suzuki et al., 2010) or can only be classified against existing databases (Aytan-Aktug et al., 2022).

538   Therefore, to streamline this process, we used taxonomic associations as a
539   means of linking bacteria with their corresponding MGEs using the stringent
540   filtering/identification criteria. Based on the already established stringent cutoffs for
541   plasmid/phage predictions, the original MGE predictions from PathoFact were used
542   without any additional processing and the taxonomic classifications from Kraken2 were
543   used to assign putative hosts. Finally, to obtain the gene copy number and
544   transcriptome expression levels, both metagenomic and metatranscriptomic reads were
545   independently mapped to the corresponding assembly files per sample. The raw read
546   counts per contig as well as per individual ORF, as given by PathoFact, were
547   determined with the featureCounts option. The relative abundance of the ARGs was
548   calculated using the RNum_Gi method previously described by Hu et al. (Hu et al.,
549   2013).

Metaproteomics and data analyses

551   Raw mass spectrometry files were converted to MGF format using MSconvert
552   (Chambers et al., 2012) with default parameters. The metaproteomic searches were
553   performed using SearchGUI / PeptideShaker (Vaudel et al., 2015) for each time point.
554   To generate the databases, each predicted protein sequence file was concatenated with
555   the cRAP database of contaminants (*common Repository of Adventitious Proteins*, v
556   2012.01.01; The Global Proteome Machine) and with the human UniProtKB Reference
557   Proteome (UniProt Consortium, 2021). In addition, inverted sequences of all protein
558   entries were concatenated to the databases for the estimation of false discovery rates
559   (FDRs). The search was performed using SearchGUI-3.3.20 (Barsnes and Vaudel,
560   2018) with the X!Tandem (Langella et al., 2017), MS-GF+ (Kim and Pevzner, 2014) and
561   Comet (Eng et al., 2013) search engines using the following parameters: Trypsin was
562   used as the digestion enzyme and a maximum of two missed cleavage sites was
563   allowed. The tolerance levels for identification were 10 ppm for MS1 and 15ppm for
564   MS2. Carbamidomethylation of cysteine residues was set as a fixed modification and
565   oxidation of methionines was allowed as variable modification. Peptides with a length
566   between 7 and 60 amino acids and with a charge state composed between +2 and +4
567   were considered for identification. The results from SearchGUI were merged using

568 PeptideShaker-1.16.45 (Vaudel et al., 2015) and all identifications were filtered in order
569 to achieve a peptide and protein FDR of 1%.

570   Each predicted protein sequence corresponded to the predicted ORFs generated
571 by the Prodigal (version 2.6.3) predictions included in PathoFact. As such predicted
572 protein sequences matched the ARG annotation of the ORFs as provided by PathoFact.

Multi-omic integration

574   To further improve upon the understanding of the AMR expression and assess its
575 stability across time, we estimated the normalized protein index (NPI) per gene, by
576 integrating the multi-omic data. To estimate the NPI, we first normalized the metaT
577 abundance based on per gene copy numbers obtained via the metagenomic
578 abundance:

$$NPI = \frac{Nmetaproteome}{Nmetatranscriptome \ / \ Nmetagenome}$$

579

580   This, the normalized expression of genes, yields the per copy expression of
581 ARGs within each AMR category. Subsequently, the normalized expression was used
582 to standardize the metaP abundances for those genes where the necessary data was
583 available.

MGE partition assessment

585   To assess the segregation of MGEs through AMR we determined niche regions
586 and overlap using the *nicheROVER* R package (Swanson et al., 2015). *nicheROVER*
587 uses Bayesian methods to calculate niche regions and pairwise niche overlap using
588 multidimensional niche indicator data (i.e. stable isotopes, environmental variables). As
589 such, using AMR as the indicator data, we extended the application of *nicheRover* to
590 calculate the probability for the size of the niche area of one MGE inside that of the
591 other, and vice versa. We calculated the segregation size estimate for each MGE and
592 additionally generated the posterior distributions of μ (population mean) for each AMR
593 category in all omics. We further computed the niche overlap estimates between MGEs
594 with a 95% confidence interval over 10 000 iterations.

595 Data analysis

596   Figures for the study including visualizations derived from the taxonomic and
597 functional analyses were created using version 3.6 of the R statistical software package
598 (Team and Others, 2013). A paired two-way ANOVA (Analysis of Variance, accounting
599 for MGEs and AMR, or taxa and AMR) within the *nlme* package was used for identifying
600 statistically significant differences. Tripartite and Bipartite networks were generated
601 using the *SpiecEasi* (Kurtz et al., 2015) R package where a weighted adjacency matrix
602 was generated using the Meinhausen and Buhlmann (*mb*) algorithm, with a nlambda of
603 40, and lambda minimum ratio at 0.001. The analyses were bootsrapped with n=999 to
604 avoid overfitting, autocorrelations and false network associations. The network was
605 further refined, selecting for positive edges, with a degree greater than the mean-degree
606 of the initial network. Additionally, edges with a correlation value greater than 0.6 were
607 retained where the associated significance was below an adjusted p-value <0.05. The
608 *igraph (Csardi and Nepusz, 2006)* package was used in R to render the graphics for the
609 network. All code for visualization and analysis is available at: https://git-
610 r3lab.uni.lu/laura.denies/lao_scripts.

611

Data availability

613   The genomic FASTQ files from this work are publicly available at NCBI
614 BioProject PRJNA230567. Metaproteomic data are publicly available at the PRIDE
615 database under accession number PXD013655.

616

Code availability

618   The open-source tools and algorithms used for the data analyses are reported in
619 the Methods section, including relevant flags used for the various tools. Additionally,
620 custom code for further analysis and generation of the figures can be found at:
621 https://git-r3lab.uni.lu/laura.denies/lao_scripts

622

Funding

629   Acknowledgements

636   Figures

637   Figure 1. Longitudinal metagenomic and metatranscriptomic assessment of AMR

638   a) ARG relative abundances over time within the BWWTP. b) AMR categories at
639   various timepoints categorized in 4 distinct groups based on presence/absence: Core
640   (all timepoints), Prevalent (>75% of timepoints), Moderate (50-75% of timepoints) and
641   Rare (< 50% of all timepoints). c) Relative abundance levels of expressed AMR
642   categories over time within the BWWTP. Colors of all panels correspond to the AMR
643   categories

644

645   Figure 2. Microbial population-linked AMR

646   a) Longitudinal ARG relative abundance levels linked to their corresponding microbial
647   taxa (order level). Colors correspond to AMR categories. b) Relative abundance of AMR
648   categories linked to *Candidatus* Microthrix parvicella with colors corresponding to AMR
649   categories. c) Bi-partite network depicting co-occurrence patterns of individual
650   antimicrobial resistance genes (ARGs) and microbial taxa on genus level. Nodes
651   represent taxa or ARG with the node size representing the number of connections. The
652   size of the edges represent the strength of interaction between the nodes.

653

654   Figure 3. Assessment of AMR associated with clinical pathogens

655 ARG relative abundances encoded and expressed by clinical pathogens over time

656 within the BWWTP, with colors corresponding to the identified pathogens.

657

658 Figure 4. MGE-derived AMR within the BWWTP resistome

659 a) Overall relative abundance of MGEs encoding ARGs. Contribution of plasmids to

660 AMR (average of 10.8% of all ARGs) was found significantly increased compared to

661 phages (average of 6.8% of all ARGs) (*adj.p* < 0.05, One-way ANOVA). Colors depict

662 the different MGE predictions (phage, plasmid, ambiguous) b) Boxplots depicting

663 significant (*adj.p* < 0.05, Two-way ANOVA) differential abundances of ARGs encoded

664 by plasmids (blue) vs phages (green). c) Relative abundance of the 6 significantly

665 different AMR categories encoded on phages over time, with colors corresponding to

666 AMR categories. d) Relative abundance of the 6 significantly different AMR categories

667 encoded on plasmids over time, with colors corresponding to AMR categories.

668

669 Figure 5 Taxonomic affiliations of MGE-derived resistance genes

670 a) Boxplot depicting significant differential abundance (*adj.p* < 0.05, Two-way ANOVA)

671 of ARGs expressed in plasmids vs phages. b) Tripartite network assessing the

672 association of MGE-derived ARGs with the microbial taxa. Thickness of the lines

673 representing potential niche-partitioning of the AMR category to one MGE over the

674 other. Color of the line representing which MGE the AMR is linked to: green (phage),

675 blue (plasmid) or black (both phage and plasmid). Asterisk denominates taxonomic

676 orders which include known clinical pathogens. c) Alluvial plot depicting the mean

677 abundance (log10) of MGE-derived ARGs encoded (metagenome) and/or expressed

678 (metagenome) by clinical pathogens. Colors of all panels correspond to the MGEs and

679 AMR categories.

680

681 Figure 6. Integrative multi-omic assessment of AMR

682 a) metagenomic and metatranscriptomic normalized protein levels linked to AMR within

683 the WTTP over time. b)Tripartite network assessing the normalized protein levels

684 derived from MGEs and associated taxa. Boxplots depicting significant differential (*adj.p*

685 *< 0.05,* Two-way ANOVA) abundance of aminoglycoside resistance in plasmid versus

686   phage in *Candidatus* Microthrix parvicella as well as overall. Colors of all panels
687   correspond to the MGEs and AMR categories.

688

689   Figure 7. Separation of MGE-derived AMR within the BWWTP.

690   A graphical summary highlighting AMR categories found significantly increased in
691   phage versus plasmid in all three omes.

692

693   Figure 8. Identification of ARGs and contextualization of MGEs in relation to taxa .

694   A schematic diagram depicting the bioinformatic workflow to identify ARGs and the
695   subsequent contextualization of MGEs in relation to microbial taxa. The green features
696   represent the different tools and pipelines used while the red features highlight the data
697   used and generated in this process.

698

699   Figure 1-figure supplement 1. Expression levels of individual ARGs

700   Expression levels of individual ARGs contributing to peptide resistance over time within
701   the BWWTP, with colors corresponding to the individual ARGs.

702

703   Figure 2-figure supplement 1. Taxonomic diversity of AMR

704   The plot indicates the number of taxa (order level) in which the corresponding AMR
705   categories are identified. Numbers of taxa are highlighted at the top of each bar, with
706   colors corresponding to the AMR categories, as visualized by the same colors in all
707   figures, on the x-axis.

708

709   Figure 2-figure supplement 2. Expressed AMR categories of *Candidatus* Microthrix
710   parvicella

711   Expression levels of AMR categories linked to *Candidatus* Microthrix parvicella over
712   time. Colors correspond to the AMR categories.

713

714   Figure 4-figure supplement 1. Partitioning of MGEs through AMR

715   The boxplots indicate the niche sizes (left) for the MGEs (plasmids and phages) based
716   on metagenomic assessment. Niche plots (right) reveal that plasmids (blue) tend to

differentiate from phages (green) based on their capacity to encode for aminoglycoside resistance.

Figure 4-figure supplement 2. Chromosomal-derived AMR

Alluvial plot depicting relative abundances of chromosomal-derived ARGs over time, with colors depicting the AMR categories.

Figure 5-figure supplement 1. Differential ARG abundance in MGEs

The barplot reports the log2foldchange of the relative abundance of AMR categories over time in MGEs (plasmid versus phage) in: a) the general microbial population, b) *M. parvicella,* c) *Pseudomonas* spp. And d) *Comamonas* spp. Colors of all panels correspond to the AMR categories

Figure 5-figure supplement 2. Expression of AMR categories in MGEs

The barplot reports the expression levels of AMR categories over time in MGEs (plasmid versus phage) in: a) Acidimicrobiales, and b) Burkholderiales. Colors of all panels correspond to the AMR categories.

Figure 6-figure supplement 1. AMR protein abundances

Barplot depicting protein abundances of various AMR categories over time. Colors correspond to the AMR categories.

References

Aarestrup FM, Woolhouse MEJ. 2020. Using sewage for surveillance of antimicrobial resistance. *Science* **367**:630–632.

Alcock BP, Raphenya AR, Lau TTY, Tsang KK, Bouchard M, Edalatmand A, Huynh W, Nguyen A-LV, Cheng AA, Liu S, Min SY, Miroshnichenko A, Tran H-K, Werfalli RE, Nasir JA, Oloni M, Speicher DJ, Florescu A, Singh B, Faltyn M, Hernandez-Koutoucheva A, Sharma AN, Bordeleau E, Pawlowski AC, Zubyk HL, Dooley D, Griffiths E, Maguire F, Winsor GL, Beiko RG, Brinkman FSL, Hsiao WWL, Domselaar GV, McArthur AG. 2020. CARD 2020: antibiotic resistome surveillance with the comprehensive antibiotic resistance database. *Nucleic Acids Res* **48**:D517–D525.

Alexander J, Hembach N, Schwartz T. 2020a. Evaluation of antibiotic resistance dissemination by wastewater treatment plant effluents with different catchment areas in Germany. *Sci Rep* **10**:8952.

751 Alexander J, Hembach N, Schwartz T. 2020b. Evaluation of antibiotic resistance dissemination
752   by wastewater treatment plant effluents with different catchment areas in Germany. *Sci Rep*
753   **10**:8952.
754 Aytan-Aktug D, Clausen PTLC, Szarvas J, Munk P, Otani S, Nguyen M, Davis JJ, Lund O,
755   Aarestrup FM. 2022. PlasmidHostFinder: Prediction of Plasmid Hosts Using Random
756   Forest. *mSystems* **7**:e0118021.
757 Baquero F, Martínez J-L, Cantón R. 2008. Antibiotics and antibiotic resistance in water
758   environments. *Curr Opin Biotechnol* **19**:260–265.
759 Barsnes H, Vaudel M. 2018. SearchGUI: A Highly Adaptable Common Interface for Proteomics
760   Search and de Novo Engines. *J Proteome Res* **17**:2552–2555.
761 Beceiro A, Tomás M, Bou G. 2013. Antimicrobial resistance and virulence: a successful or
762   deleterious association in the bacterial world? *Clin Microbiol Rev* **26**:185–230.
763 Ben Said L, Emond-Rheault J-G, Soltani S, Telhig S, Zirah S, Rebuffat S, Diarra MS, Goodridge
764   L, Levesque RC, Fliss I. 2020. Phenomic and genomic approaches to studying the
765   inhibition of multiresistant Salmonella enterica by microcin J25. *Environ Microbiol* **22**:2907–
766   2920.
767 Blake DP, Hillman K, Fenlon DR, Low JC. 2003. Transfer of antibiotic resistance between
768   commensal and pathogenic members of the Enterobacteriaceae under ileal conditions. *J*
769   *Appl Microbiol* **95**:428–436.
770 Bland C, Ramsey TL, Sabree F, Lowe M, Brown K, Kyrpides NC, Hugenholtz P. 2007. CRISPR
771   recognition tool (CRT): a tool for automatic detection of clustered regularly interspaced
772   palindromic repeats. *BMC Bioinformatics* **8**:209.
773 Bonilla AR, Muniz KP. 2009. Antibiotic Resistance: Causes and Risk Factors, Mechanisms and
774   Alternatives. Nova Science Publishers.
775 Bouanchaud DH, Chabbert YA. 1971. The problems of drug-resistant pathogenic bacteria.
776   Practical effectiveness of agents curing R factors and plasmids. *Ann N Y Acad Sci*
777   **182**:305–311.
778 Brinkac L, Voorhies A, Gomez A, Nelson KE. 2017. The Threat of Antimicrobial Resistance on
779   the Human Microbiome. *Microb Ecol* **74**:1001–1008.
780 Brogan DM, Mossialos E. 2016. A critical analysis of the review on antimicrobial resistance
781   report and the infectious disease financing facility. *Global Health* **12**:8.
782 Buckner MMC, Ciusa ML, Piddock LJV. 2018. Strategies to combat antimicrobial resistance:
783   anti-plasmid and plasmid curing. *FEMS Microbiol Rev* **42**:781–804.
784 Calero-Cáceres W, Melgarejo A, Colomer-Lluch M, Stoll C, Lucena F, Jofre J, Muniesa M.
785   2014. Sludge as a potential important source of antibiotic resistance genes in both the
786   bacterial and bacteriophage fractions. *Environ Sci Technol* **48**:7602–7611.
787 Calusinska M, Goux X, Fossépré M, Muller EEL, Wilmes P, Delfosse P. 2018. A year of
788   monitoring 20 mesophilic full-scale bioreactors reveals the existence of stable but different
789   core microbiomes in bio-waste and wastewater anaerobic digestion systems. *Biotechnol*
790   *Biofuels* **11**:1–19.
791 Cameron DE, Collins JJ. 2014. Tunable protein degradation in bacteria. *Nat Biotechnol*
792   **32**:1276–1281.
793 Carattoli A. 2013. Plasmids and the spread of resistance. *Int J Med Microbiol* **303**:298–304.
794 Chambers MC, Maclean B, Burke R, Amodei D, Ruderman DL, Neumann S, Gatto L, Fischer B,
795   Pratt B, Egertson J, Hoff K, Kessner D, Tasman N, Shulman N, Frewen B, Baker TA,
796   Brusniak M-Y, Paulse C, Creasy D, Flashner L, Kani K, Moulding C, Seymour SL, Nuwaysir
797   LM, Lefebvre B, Kuhlmann F, Roark J, Rainer P, Detlev S, Hemenway T, Huhmer A,
798   Langridge J, Connolly B, Chadick T, Holly K, Eckels J, Deutsch EW, Moritz RL, Katz JE,
799   Agus DB, MacCoss M, Tabb DL, Mallick P. 2012. A cross-platform toolkit for mass
800   spectrometry and proteomics. *Nat Biotechnol* **30**:918–920.
801 Chen B, Yang Y, Liang X, Yu K, Zhang T, Li X. 2013. Metagenomic profiles of antibiotic

802   resistance genes (ARGs) between human impacted estuary and deep ocean sediments.
803   *Environ Sci Technol* **47**:12753–12760.

804 Che Y, Xia Y, Liu L, Li A-D, Yang Y, Zhang T. 2019. Mobile antibiotic resistome in wastewater
805   treatment plants revealed by Nanopore metagenomic sequencing. *Microbiome* **7**:44.

806 Chiang YN, Penadés JR, Chen J. 2019. Genetic transduction by phages and chromosomal
807   islands: The new and noncanonical. *PLoS Pathog* **15**:e1007878.

808 Csardi G, Nepusz T. 2006. The igraph software package for complex network research.
809   *InterJournal, Complex Systems* **1695**:1–9.

810 Datta N, Hughes VM. 1983. Plasmids of the same Inc groups in Enterobacteria before and after
811   the medical use of antibiotics. *Nature* **306**:616–617.

812 Delgado MA, Vincent PA, Farías RN, Salomón RA. 2005. YojI of Escherichia coli functions as a
813   microcin J25 efflux pump. *J Bacteriol* **187**:3465–3470.

814 de Nies L, Lopes S, Busi SB, Galata V, Heintz-Buschart A, Laczny CC, May P, Wilmes P. 2021.
815   PathoFact: a pipeline for the prediction of virulence factors and antimicrobial resistance
816   genes in metagenomic data. *Microbiome* **9**:49.

817 Dubnau D, Grandi G, Grandi R, Gryczan TJ, Hahn J, Kozloff Y, Shivakumar AG. 1981.
818   Regulation of Plasmid Specified MLS-Resistance in Bacillus subtilis by Conformational
819   Alteration of RNA Structure In: Levy SB, Clowes RC, Koenig EL, editors. Molecular Biology,
820   Pathogenicity, and Ecology of Bacterial Plasmids. Boston, MA: Springer US. pp. 157–167.

821 Eng JK, Jahan TA, Hoopmann MR. 2013. Comet: an open-source MS/MS sequence database
822   search tool. *Proteomics* **13**:22–24.

823 Fouz N, Pangesti KNA, Yasir M, Al-Malki AL, Azhar EI, Hill-Cawthorne GA, Abd El Ghany M.
824   2020. The Contribution of Wastewater to the Transmission of Antimicrobial Resistance in
825   the Environment: Implications of Mass Gathering Settings. *Trop Med Infect Dis* **5**.
826   doi:10.3390/tropicalmed5010033

827 Frost I, Smith WPJ, Mitri S, Millan AS, Davit Y, Osborne JM, Pitt-Francis JM, MacLean RC,
828   Foster KR. 2018. Cooperation, competition and antibiotic resistance in bacterial colonies.
829   *ISME J* **12**:1582–1593.

830 Galimand M, Courvalin P, Lambert T. 2003. Plasmid-mediated high-level resistance to
831   aminoglycosides in Enterobacteriaceae due to 16S rRNA methylation. *Antimicrob Agents*
832   *Chemother* **47**:2565–2571.

833 Han X, Du X-D, Southey L, Bulach DM, Seemann T, Yan X-X, Bannam TL, Rood JI. 2015.
834   Functional Analysis of a Bacitracin Resistance Determinant Located on ICECp1, a Novel
835   Tn916-Like Element from a Conjugative Plasmid in Clostridium perfringens. *Antimicrob*
836   *Agents Chemother* **59**:6855–6865.

837 Hendriksen RS, Munk P, Njage P, van Bunnik B, McNally L, Lukjancenko O, Röder T,
838   Nieuwenhuijse D, Pedersen SK, Kjeldgaard J, Kaas RS, Clausen PTLC, Vogt JK,
839   Leekitcharoenphon P, van de Schans MGM, Zuidema T, de Roda Husman AM,
840   Rasmussen S, Petersen B, Global Sewage Surveillance project consortium, Amid C,
841   Cochrane G, Sicheritz-Ponten T, Schmitt H, Alvarez JRM, Aidara-Kane A, Pamp SJ, Lund
842   O, Hald T, Woolhouse M, Koopmans MP, Vigre H, Petersen TN, Aarestrup FM. 2019.
843   Global monitoring of antimicrobial resistance based on metagenomics analyses of urban
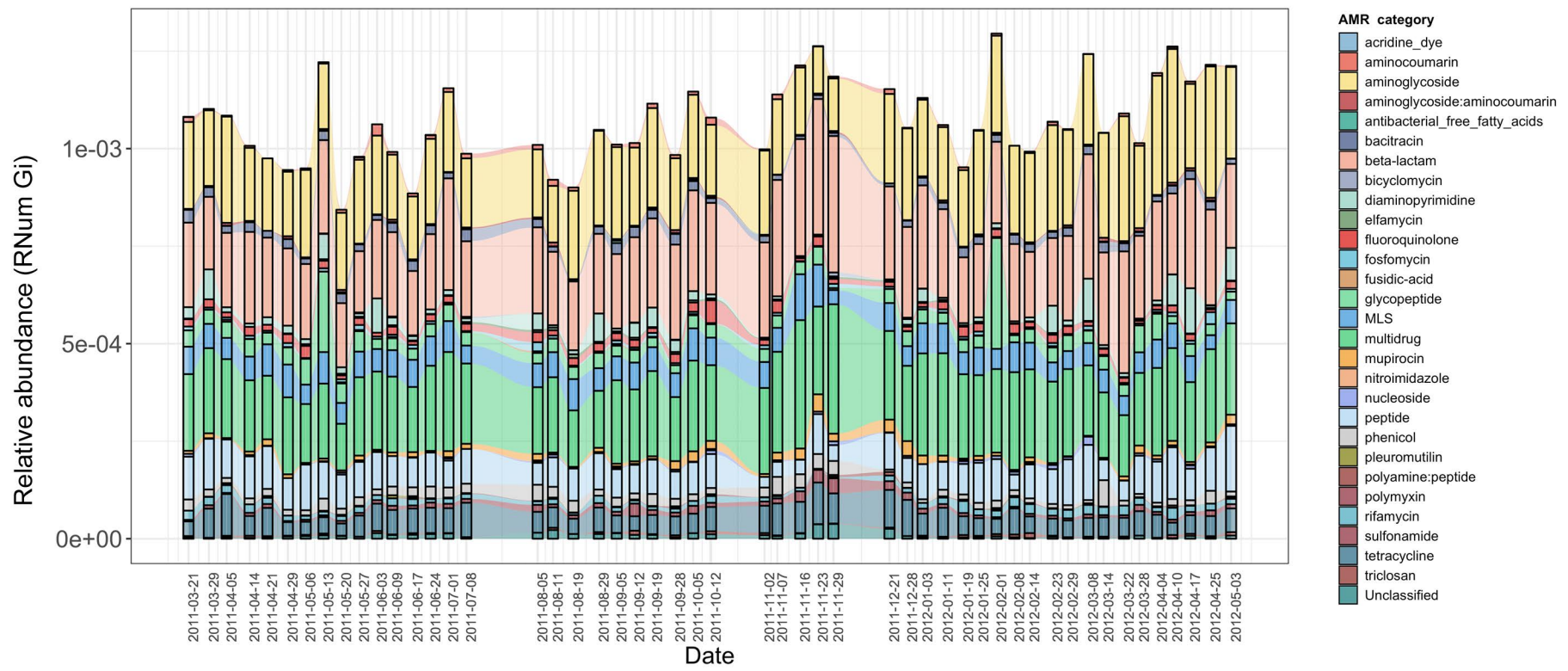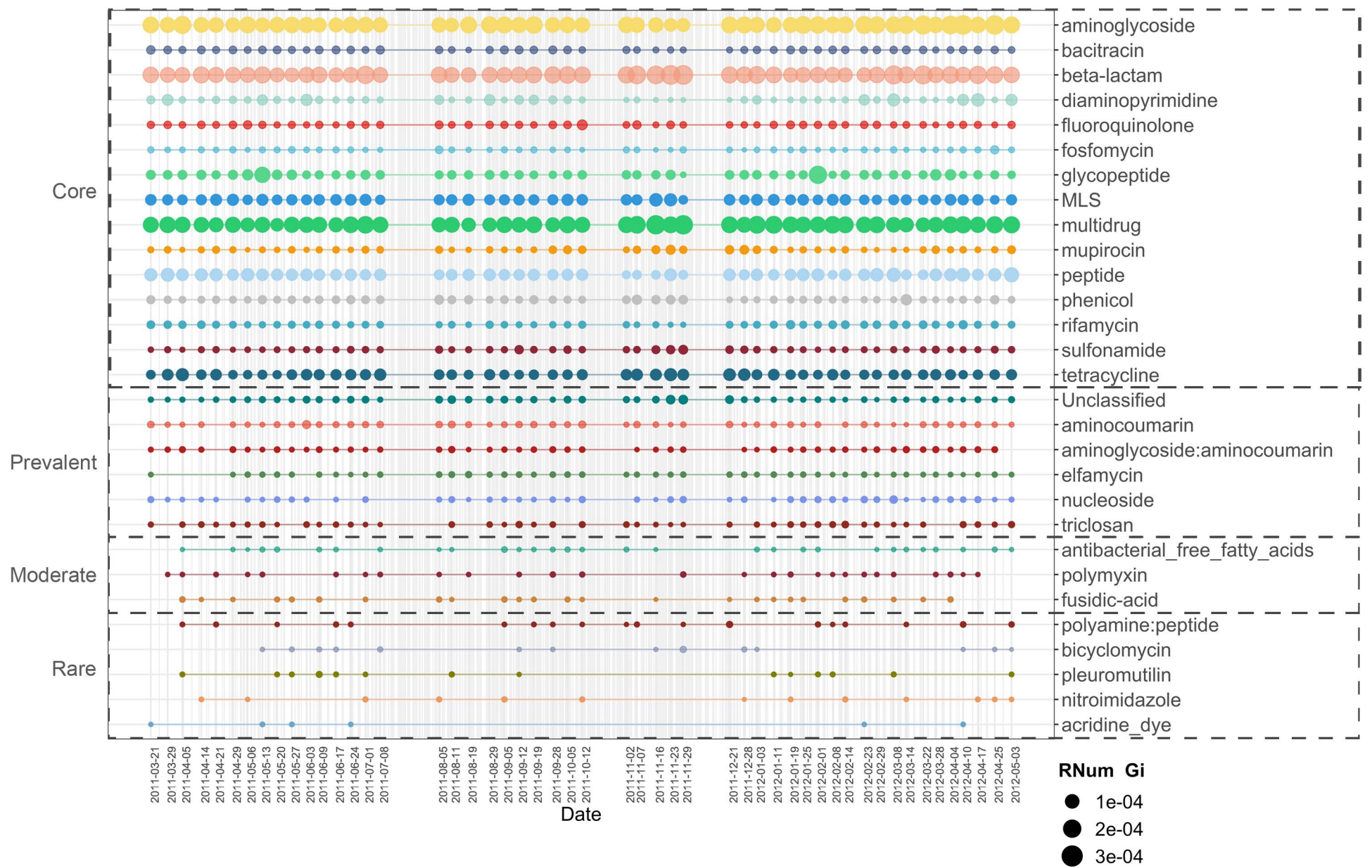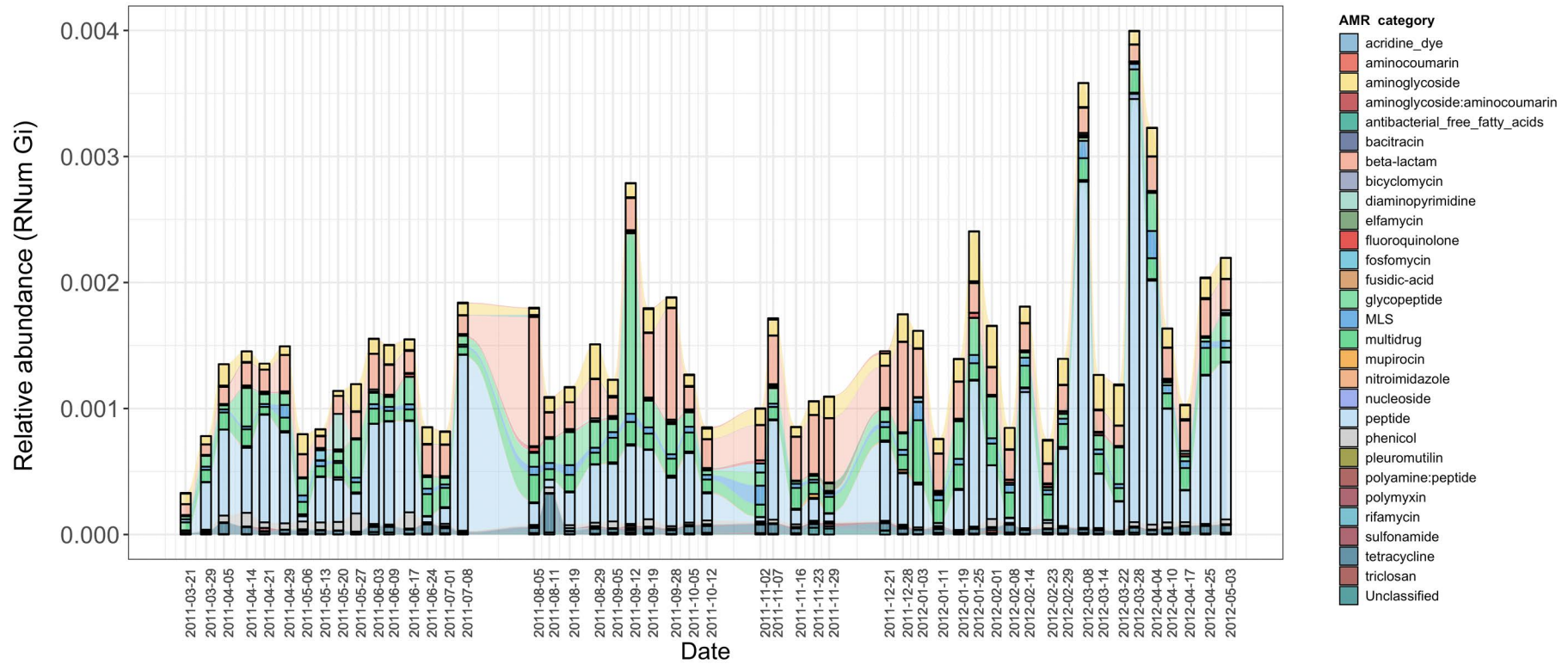844   sewage. *Nat Commun* **10**:1124.

845 Herold M, d'Hérouël AF, May P, Delogu F, Wienecke-Baldacchino A, Tapp J, Walczak C,
846   Wilmes P, Cauchie H-M, Fournier G, Ogorzaly L. 2021. Genome Sequencing of SARS-
847   CoV-2 Allows Monitoring of Variants of Concern through Wastewater. *Water* **13**:3018.

848 Herold M, Martínez Arbas S, Narayanasamy S, Sheik AR, Kleine-Borgmann LAK, Lebrun LA,
849   Kunath BJ, Roume H, Bessarab I, Williams RBH, Gillece JD, Schupp JM, Keim PS, Jäger
850   C, Hoopmann MR, Moritz RL, Ye Y, Li S, Tang H, Heintz-Buschart A, May P, Muller EEL,
851   Laczny CC, Wilmes P. 2020. Integration of time-series meta-omics data reveals how
852   microbial ecosystems respond to disturbance. *Nat Commun* **11**:5281.
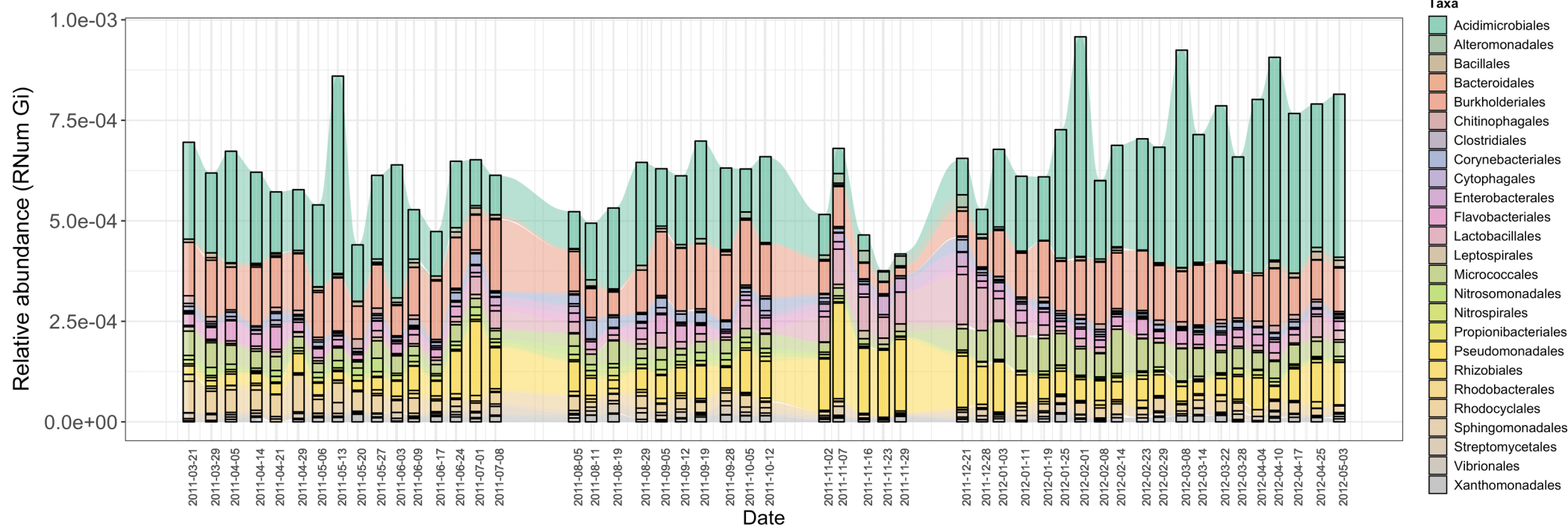
853 Hiller CX, Hübner U, Fajnorova S, Schwartz T, Drewes JE. 2019. Antibiotic microbial resistance
854   (AMR) removal efficiencies by conventional and advanced wastewater treatment
855   processes: A review. *Sci Total Environ* **685**:596–608.
856 Hu Y, Yang X, Qin J, Lu N, Cheng G, Wu N, Pan Y, Li J, Zhu L, Wang X, Meng Z, Zhao F, Liu
857   D, Ma J, Qin N, Xiang C, Xiao Y, Li L, Yang H, Wang J, Yang R, Gao GF, Wang J, Zhu B.
858   2013. Metagenome-wide analysis of antibiotic resistance genes in a large cohort of human
859   gut microbiota. *Nat Commun* **4**:2151.
860 Kim S, Pevzner PA. 2014. MS-GF+ makes progress towards a universal database search tool
861   for proteomics. *Nat Commun* **5**:5277.
862 Kurtz ZD, Müller CL, Miraldi ER, Littman DR, Blaser MJ, Bonneau RA. 2015. Sparse and
863   compositionally robust inference of microbial ecological networks. *PLoS Comput Biol*
864   **11**:e1004226.
865 Kwak Y-K, Colque P, Byfors S, Giske CG, Möllby R, Kühn I. 2015. Surveillance of antimicrobial
866   resistance among Escherichia coli in wastewater in Stockholm during 1 year: does it reflect
867   the resistance trends in the society? *Int J Antimicrob Agents* **45**:25–32.
868 Langella O, Valot B, Balliau T, Blein-Nicolas M, Bonhomme L, Zivy M. 2017. X!TandemPipeline:
869   A Tool to Manage Sequence Redundancy for Protein Inference and Phosphosite
870   Identification. *J Proteome Res* **16**:494–503.
871 Li D, Liu C-M, Luo R, Sadakane K, Lam T-W. 2015. MEGAHIT: an ultra-fast single-node
872   solution for large and complex metagenomics assembly via succinct de Bruijn graph.
873   *Bioinformatics* **31**:1674–1676.
874 Lieberman-Aiden E, van Berkum NL, Williams L, Imakaev M, Ragoczy T, Telling A, Amit I,
875   Lajoie BR, Sabo PJ, Dorschner MO, Sandstrom R, Bernstein B, Bender MA, Groudine M,
876   Gnirke A, Stamatoyannopoulos J, Mirny LA, Lander ES, Dekker J. 2009. Comprehensive
877   mapping of long-range interactions reveals folding principles of the human genome.
878   *Science* **326**:289–293.
879 Li Q, Chang W, Zhang H, Hu D, Wang X. 2019. The Role of Plasmids in the Multiple Antibiotic
880   Resistance Transfer in ESBLs-Producing Escherichia coli Isolated From Wastewater
881   Treatment Plants. *Front Microbiol* **10**:633.
882 Li R, Xie M, Dong N, Lin D, Yang X, Wong MHY, Chan EW-C, Chen S. 2018. Efficient
883   generation of complete sequences of MDR-encoding plasmids by rapid assembly of
884   MinION barcoding sequencing data. *Gigascience* **7**:1–9.
885 Lood R, Ertürk G, Mattiasson B. 2017. Revisiting Antibiotic Resistance Spreading in Wastewater
886   Treatment Plants - Bacteriophages as a Much Neglected Potential Transmission Vehicle.
887   *Front Microbiol* **8**:2298.
888 MacLean RC, San Millan A. 2019. The evolution of antibiotic resistance. *Science* **365**:1082–
889   1083.
890 Mahoney AR, Safaee MM, Wuest WM, Furst AL. 2021. The silent pandemic: Emergent
891   antibiotic resistances following the global response to SARS-CoV-2. *iScience* **24**:102304.
892 Martínez Arbas S, Narayanasamy S, Herold M, Lebrun LA, Hoopmann MR, Li S, Lam TJ,
893   Kunath BJ, Hicks ND, Liu CM, Price LB, Laczny CC, Gillece JD, Schupp JM, Keim PS,
894   Moritz RL, Faust K, Tang H, Ye Y, Skupin A, May P, Muller EEL, Wilmes P. 2021. Roles of
895   bacteriophages, plasmids and CRISPR immunity in microbial community dynamics
896   revealed using time-series integrated meta-omics. *Nat Microbiol* **6**:123–135.
897 Maximilian O. Press, Wiser AH, Kronenberg ZN, Langford KW, Shakya M, Lo C-C, Mueller KA,
898   Sullivan ST, Chain PSG, Liachko I. 2017. Hi-C deconvolution of a human gut microbiome
899   yields high-quality draft genomes and reveals plasmid-genome interactions. *bioRxiv*.
900   doi:10.1101/198713
901 Munck C, Albertsen M, Telke A, Ellabaan M, Nielsen PH, Sommer MOA. 2015. Limited
902   dissemination of the wastewater treatment plant core resistome. *Nat Commun* **6**:8452.
903 Nadeem SF, Gohar UF, Tahir SF, Mukhtar H, Pornpukdeewattana S, Nukthamna P, Moula Ali

904   AM, Bavisetty SCB, Massa S. 2020. Antimicrobial resistance: more than 70 years of war
905   between humans and bacteria. *Crit Rev Microbiol* **46**:578–599.
906   Naimi S, Zirah S, Hammami R, Fernandez B, Rebuffat S, Fliss I. 2018. Fate and Biological
907   Activity of the Antimicrobial Lasso Peptide Microcin J25 Under Gastrointestinal Tract
908   Conditions. *Front Microbiol* **9**:1764.
909   Narayanasamy S, Jarosz Y, Muller EEL, Heintz-Buschart A, Herold M, Kaysen A, Laczny CC,
910   Pinel N, May P, Wilmes P. 2016. IMP: a pipeline for reproducible reference-independent
911   integrated metagenomic and metatranscriptomic analyses. *Genome Biol* **17**:260.
912   Newton RJ, McClary JS. 2019. The flux and impact of wastewater infrastructure microorganisms
913   on human and ecosystem health. *Curr Opin Biotechnol* **57**:145–150.
914   O'Neill J. 2014. Antimicrobial resistance: tackling a crisis for the health and wealth of nations.
915   *Review on antimicrobial resistance*.
916   Pärnänen KMM, Narciso-da-Rocha C, Kneis D, Berendonk TU, Cacace D, Do TT, Elpers C,
917   Fatta-Kassinos D, Henriques I, Jaeger T, Karkman A, Martinez JL, Michael SG, Michael-
918   Kordatou I, O'Sullivan K, Rodriguez-Mozaz S, Schwartz T, Sheng H, Sørum H, Stedtfeld
919   RD, Tiedje JM, Giustina SVD, Walsh F, Vaz-Moreira I, Virta M, Manaia CM. 2019. Antibiotic
920   resistance in European wastewater treatment plants mirrors the pattern of clinical antibiotic
921   resistance prevalence. *Sci Adv* **5**:eaau9124.
922   Parsley LC, Consuegra EJ, Kakirde KS, Land AM, Harper WF Jr, Liles MR. 2010. Identification
923   of diverse antimicrobial resistance determinants carried on bacterial, plasmid, or viral
924   metagenomes from an activated sludge microbial assemblage. *Appl Environ Microbiol*
925   **76**:3753–3757.
926   Proia L, Anzil A, Borrego C, Farrè M, Llorca M, Sanchis J, Bogaerts P, Balcázar JL, Servais P.
927   2018. Occurrence and persistence of carbapenemases genes in hospital and wastewater
928   treatment plants and propagation in the receiving river. *J Hazard Mater* **358**:33–43.
929   Razavi M, Marathe NP, Gillings MR, Flach C-F, Kristiansson E, Joakim Larsson DG. 2017.
930   Discovery of the fourth mobile sulfonamide resistance gene. *Microbiome* **5**:160.
931   Reinthaler FF, Galler H, Feierl G, Haas D, Leitner E, Mascher F, Melkes A, Posch J, Pertschy
932   B, Winter I, Himmel W, Marth E, Zarfel G. 2013. Resistance patterns of Escherichia coli
933   isolated from sewage sludge in comparison with those isolated from human patients in
934   2000 and 2009. *J Water Health* **11**:13–20.
935   Reza A, Sutton JM, Rahman KM. 2019. Effectiveness of Efflux Pump Inhibitors as Biofilm
936   Disruptors and Resistance Breakers in Gram-Negative (ESKAPEE) Bacteria. *Antibiotics*
937   *(Basel)* **8**. doi:10.3390/antibiotics8040229
938   Rodríguez-Molina D, Mang P, Schmitt H, Chifiriuc MC, Radon K, Wengenroth L. 2019. Do
939   wastewater treatment plants increase antibiotic resistant bacteria or genes in the
940   environment? Protocol for a systematic review. *Syst Rev* **8**:304.
941   Rodriguez-Mozaz S, Chamorro S, Marti E, Huerta B, Gros M, Sànchez-Melsió A, Borrego CM,
942   Barceló D, Balcázar JL. 2015. Occurrence of antibiotics and antibiotic resistance genes in
943   hospital and urban wastewaters and their impact on the receiving river. *Water Res* **69**:234–
944   242.
945   Roume H, Heintz-Buschart A, Muller EEL, Wilmes P. 2013. Sequential isolation of metabolites,
946   RNA, DNA, and proteins from the same unique sample. *Methods Enzymol* **531**:219–236.
947   Singer AC, Shaw H, Rhodes V, Hart A. 2016. Review of Antimicrobial Resistance in the
948   Environment and Its Relevance to Environmental Regulators. *Front Microbiol* **7**:1728.
949   Slizovskiy IB, Mukherjee K, Dean CJ, Boucher C, Noyes NR. 2020. Mobilization of Antibiotic
950   Resistance: Are Current Approaches for Colocalizing Resistomes and Mobilomes Useful?
951   *Front Microbiol* **11**:1376.
952   Strange JES, Leekitcharoenphon P, Møller FD, Aarestrup FM. 2021. Metagenomics analysis of
953   bacteriophages and antimicrobial resistance from global urban sewage. *Sci Rep* **11**:1600.
954   Su J-Q, An X-L, Li B, Chen Q-L, Gillings MR, Chen H, Zhang T, Zhu Y-G. 2017. Metagenomics
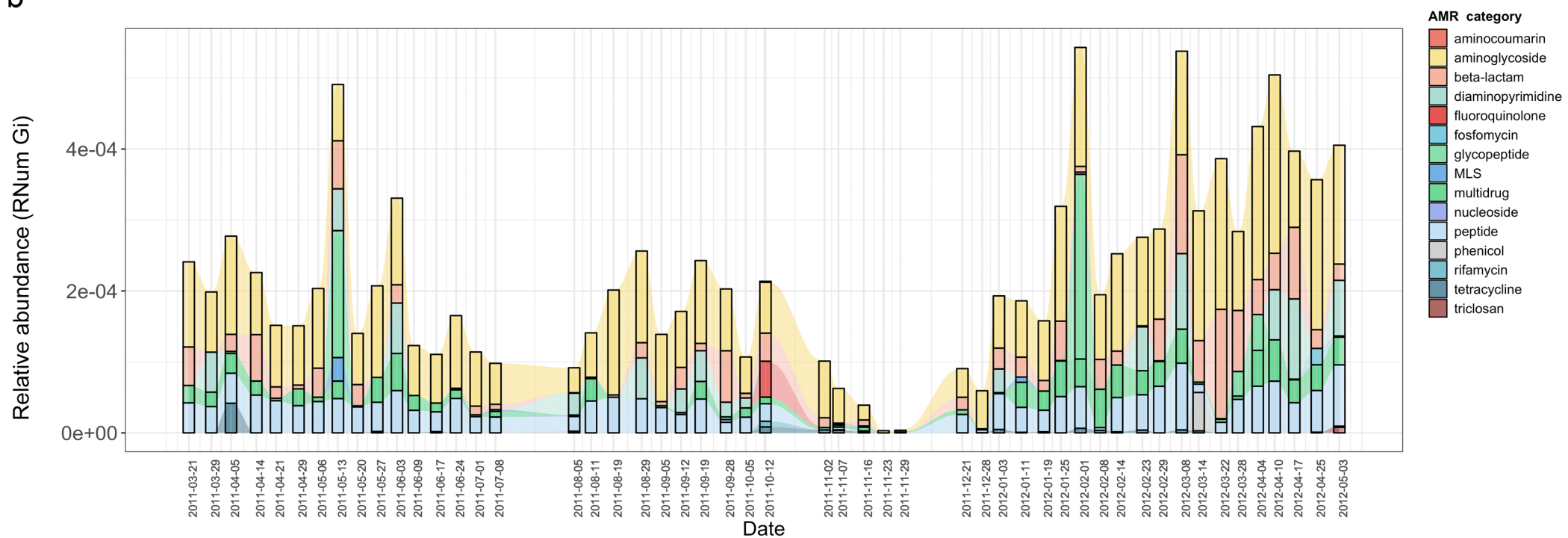
955 of urban sewage identifies an extensively shared antibiotic resistome in China. *Microbiome*
956   **5**:84.
957 Suzuki H, Yano H, Brown CJ, Top EM. 2010. Predicting plasmid promiscuity based on genomic
958   signature. *J Bacteriol* **192**:6045–6055.
959 Swanson HK, Lysy M, Power M, Stasko AD, Johnson JD, Reist JD. 2015. A new probabilistic
960   method for quantifying n-dimensional ecological niches and niche overlap. *Ecology* **96**:318–
961   324.
962 Szczepanowski R, Linke B, Krahn I, Gartemann K-H, Gützkow T, Eichler W, Pühler A, Schlüter
963   A. 2009. Detection of 140 clinically relevant antibiotic-resistance genes in the plasmid
964   metagenome of wastewater treatment plant bacteria showing reduced susceptibility to
965   selected antibiotics. *Microbiology* **155**:2306–2319.
966 Tacconelli E, Carrara E, Savoldi A, Harbarth S, Mendelson M, Monnet DL, Pulcini C, Kahlmeter
967   G, Kluytmans J, Carmeli Y, Ouellette M, Outterson K, Patel J, Cavaleri M, Cox EM,
968   Houchens CR, Grayson ML, Hansen P, Singh N, Theuretzbacher U, Magrini N, WHO
969   Pathogens Priority List Working Group. 2018. Discovery, research, and development of
970   new antibiotics: the WHO priority list of antibiotic-resistant bacteria and tuberculosis. *Lancet*
971   *Infect Dis* **18**:318–327.
972 Team RC, Others. 2013. R: A language and environment for statistical computing.
973 Torres-Barceló C. 2018. The disparate effects of bacteriophages on antibiotic-resistant bacteria.
974   *Emerg Microbes Infect* **7**:168.
975 Trinh P, Zaneveld JR, Safranek S, Rabinowitz PM. 2018. One Health Relationships Between
976   Human, Animal, and Environmental Microbiomes: A Mini-Review. *Front Public Health*
977   **6**:235.
978 Turolla A, Cattaneo M, Marazzi F, Mezzanotte V, Antonelli M. 2018. Antibiotic resistant bacteria
979   in urban sewage: Role of full-scale wastewater treatment plants on environmental
980   spreading. *Chemosphere* **191**:761–769.
981 UniProt Consortium. 2021. UniProt: the universal protein knowledgebase in 2021. *Nucleic Acids*
982   *Res* **49**:D480–D489.
983 Varrette S, Bouvry P, Cartiaux H, Georgatos F. 2014. Management of an academic HPC
984   cluster: The UL experience2014 International Conference on High Performance Computing
985   Simulation (HPCS). pp. 959–967.
986 Vaudel M, Burkhart JM, Zahedi RP, Oveland E, Berven FS, Sickmann A, Martens L, Barsnes H.
987   2015. PeptideShaker enables reanalysis of MS-derived proteomics data sets. *Nat*
988   *Biotechnol* **33**:22–24.
989 von Wintersdorff CJH, Penders J, van Niekerk JM, Mills ND, Majumder S, van Alphen LB,
990   Savelkoul PHM, Wolffs PFG. 2016. Dissemination of Antimicrobial Resistance in Microbial
991   Ecosystems through Horizontal Gene Transfer. *Front Microbiol* **7**:173.
992 Vrancianu CO, Popa LI, Bleotu C, Chifiriuc MC. 2020. Targeting Plasmids to Limit Acquisition
993   and Transmission of Antimicrobial Resistance. *Front Microbiol* **11**:761.
994 Wee BA, Muloi DM, van Bunnik BAD. 2020. Quantifying the transmission of antimicrobial
995   resistance at the human and livestock interface with genomics. *Clin Microbiol Infect*
996   **26**:1612–1616.
997 Westhaus S, Weber F-A, Schiwy S, Linnemann V, Brinkmann M, Widera M, Greve C, Janke A,
998   Hollert H, Wintgens T, Ciesek S. 2021. Detection of SARS-CoV-2 in raw and treated
999   wastewater in Germany - Suitability for COVID-19 surveillance and potential transmission
1000   risks. *Sci Total Environ* **751**:141750.
1001 Wood DE, Lu J, Langmead B. 2019. Improved metagenomic analysis with Kraken 2. *Genome*
1002   *Biol* **20**:257.
1003 Wright GD. 2007. The antibiotic resistome: the nexus of chemical and genetic diversity. *Nat Rev*
1004   *Microbiol* **5**:175–186.
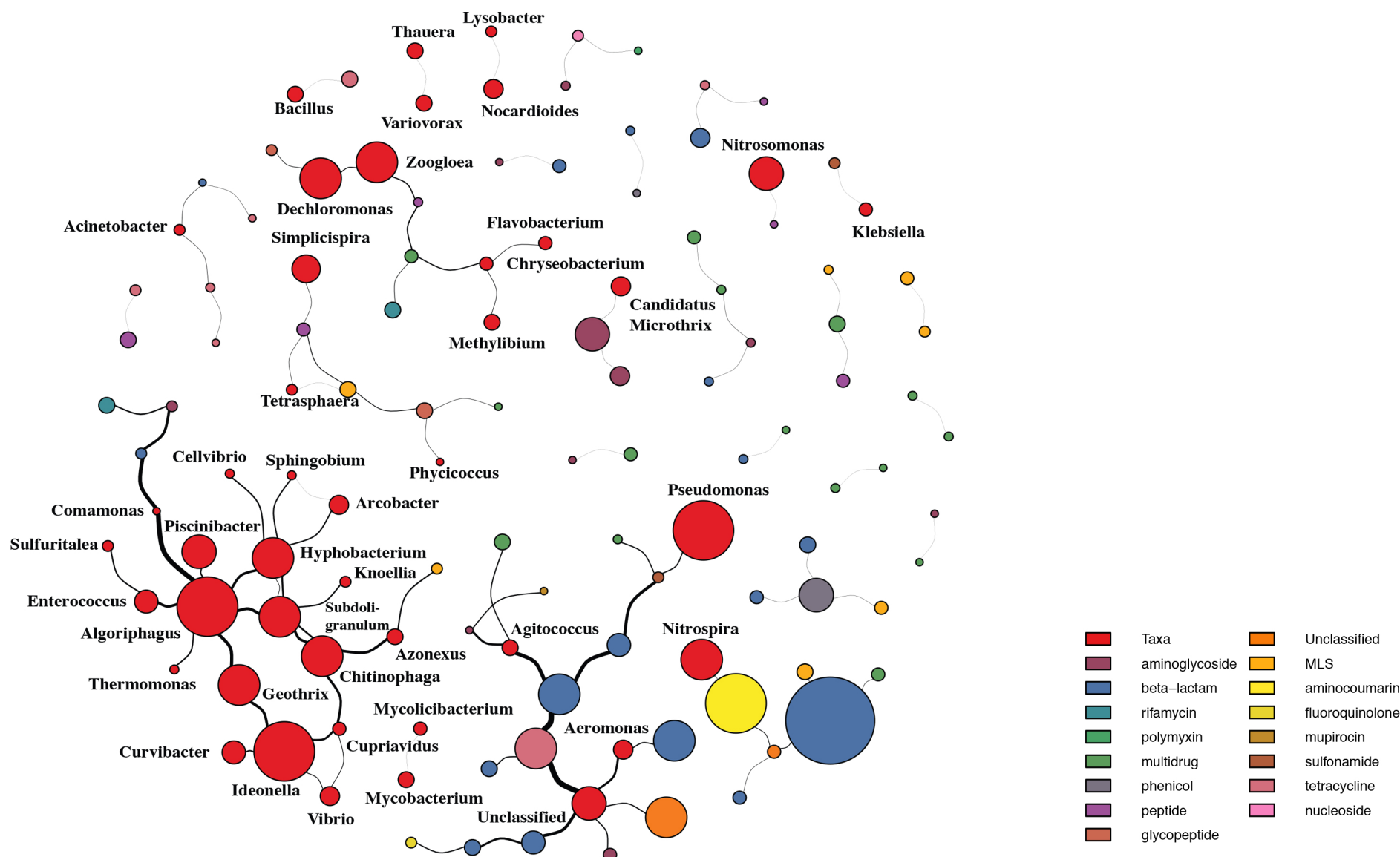
1005

a

b

c

a

aminoglycoside

bacitracin

glycopeptide

mupirocin

peptide

sulfonamide

Relative abundance (RNum Gi)

MGE prediction
- phage
- plasmid

b

phage

plasmid

fosfomycin
sulfonamide
peptide
aminoglycoside
bacitracin
MLS

Propionibacteriales
Micromonosporales
Bifidobacteriales
Micrococcales
Anaerolineales
Rhizobiales
Vibrionales
Nitrospirales
Pseudomonadales *
Marinilabiales
Aeromonadales
Pseudonocardiales
Burkholderiales
Sphingomonadales
Nitrosomonadales
Rhodocyclales
Bacillales *
Trypanosomatida
Enterobacterales *
Rhodospirillales
Mycosphaerellales
Legionellales
Cytophagales
Eggerthellales
Oceanospirillales
Chitinophagales
Acidimicrobiales
Holophagales
Rhodobacterales
Methanosarcinales
Synechococcales
Rickettsiales
Chloroflexales
Sphingobacteriales
Planctomycetales
Xanthomonadales
Alteromonadales
Flavobacteriales
Myxococcales
Corynebacteriales
Streptomycetales
Lactobacillales *
Cellvibrionales
Clostridiales
Ardenticatenales
Leptospirales
Actinomycetales *
Bacteroidales
Nostocales

c

mean

Streptococcus pneumoniae
Staphylococcus aureus
Shigella flexneri
Salmonella enterica
Pseudomonas aeruginosa
Mycobacterium tuberculosis
Klebsiella pneumoniae
Klebsiella michiganensis
Escherichia coli
Enterococcus faecium
Enterobacteriaceae
Enterobacter kobei
Enterobacter hormaechei
Acinetobacter baumannii

tetracycline
sulfonamide
peptide
multidrug
MLS
glycopeptide
fluoroquinolone
beta–lactam
bacitracin
aminoglycoside:aminocoumarin
aminoglycoside

plasmid
phage

Metatranscriptomics
Metagenomics

Taxa | AMR category | MGE prediction | 'Ome

MGE prediction
- phage
- plasmid
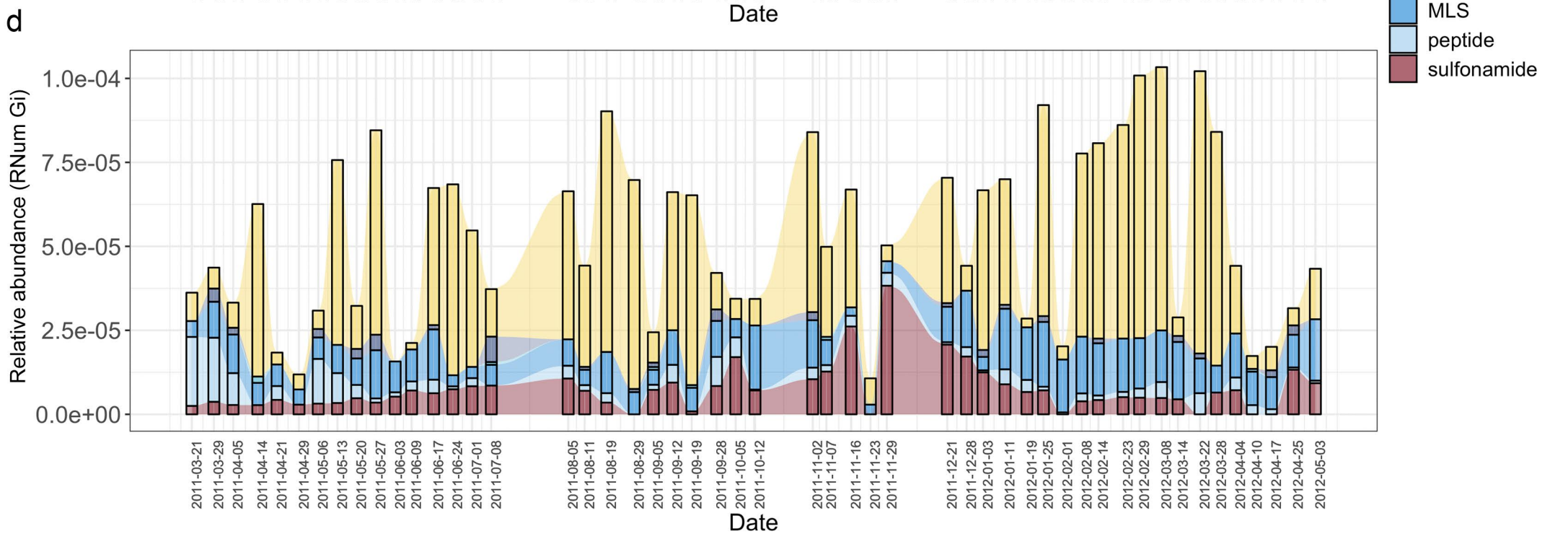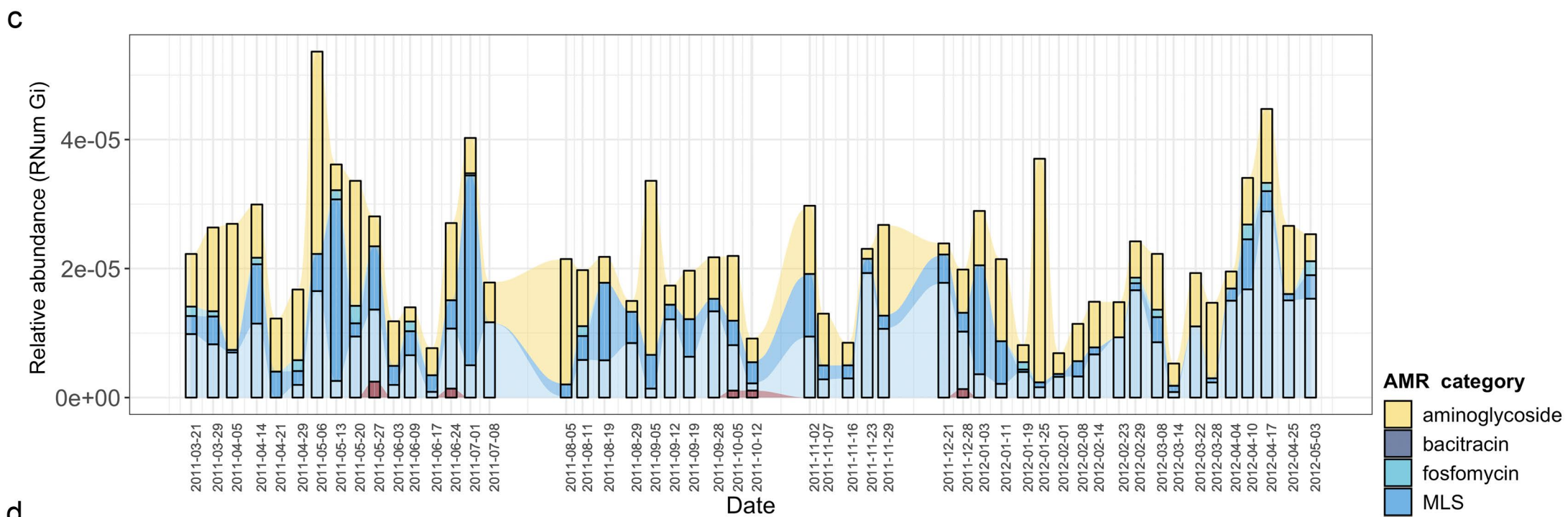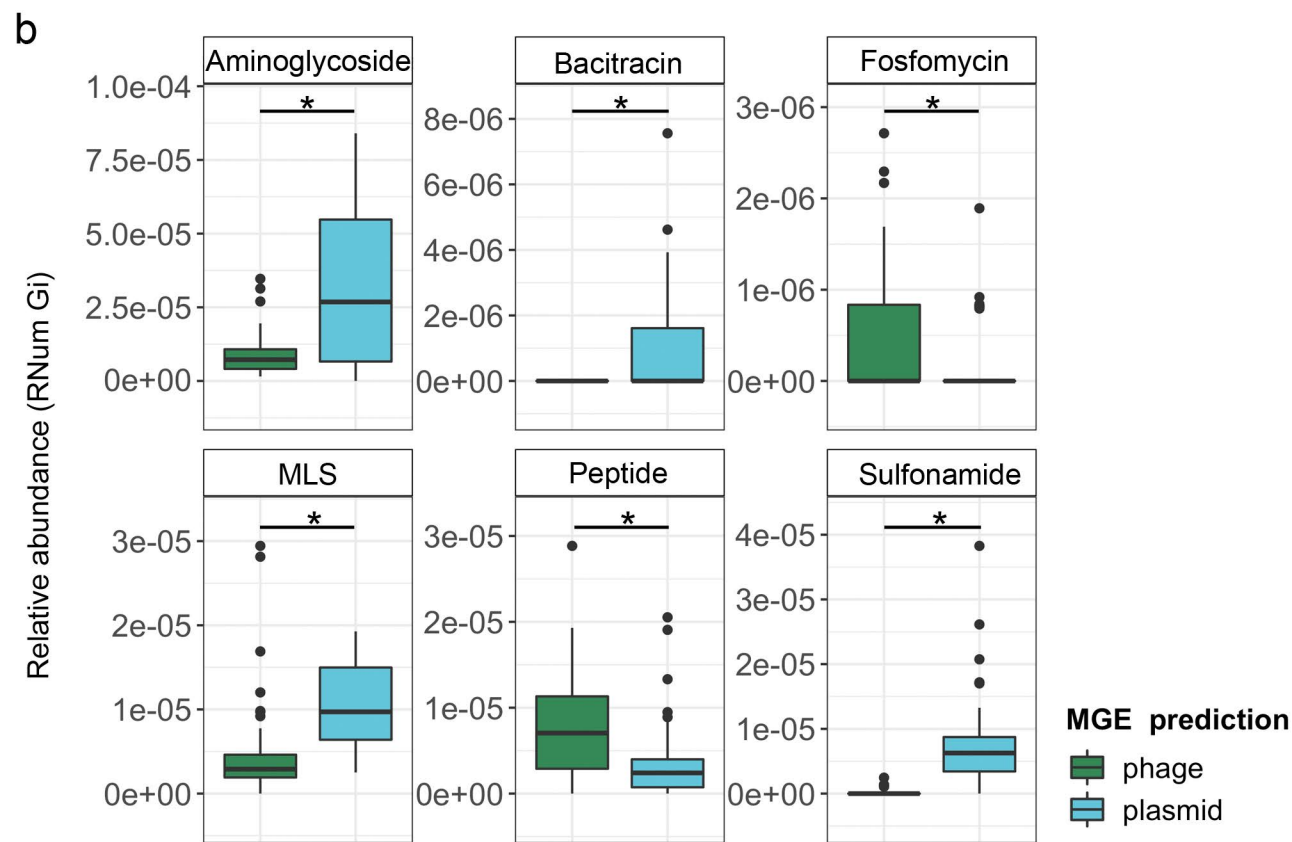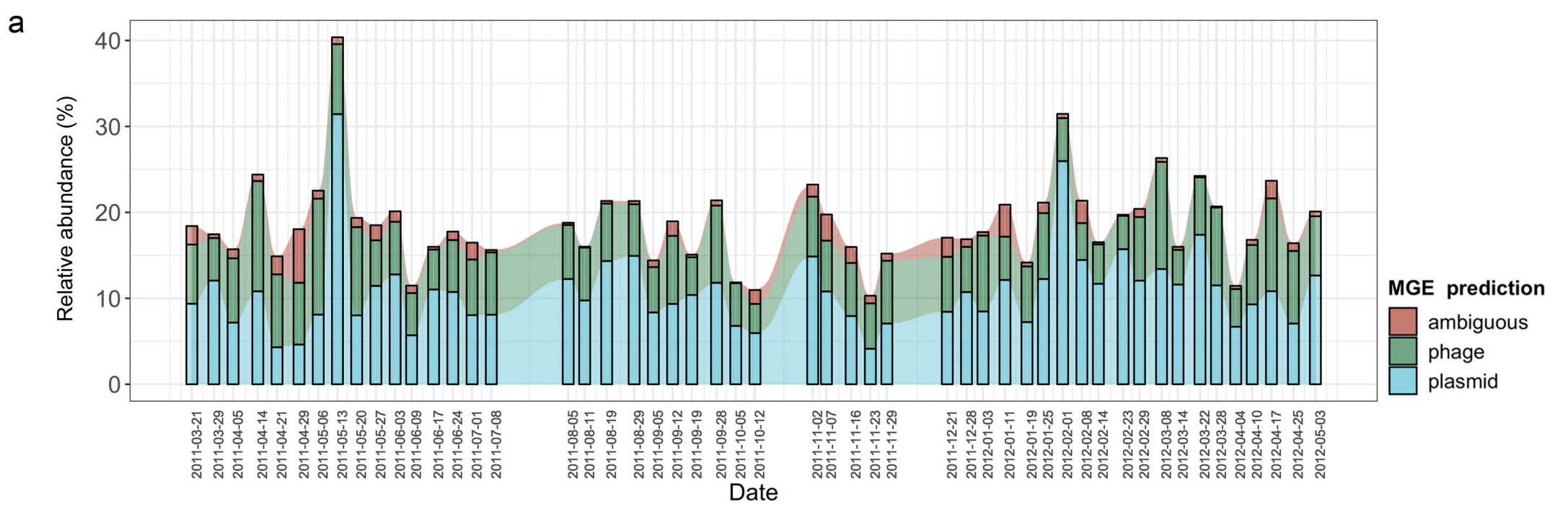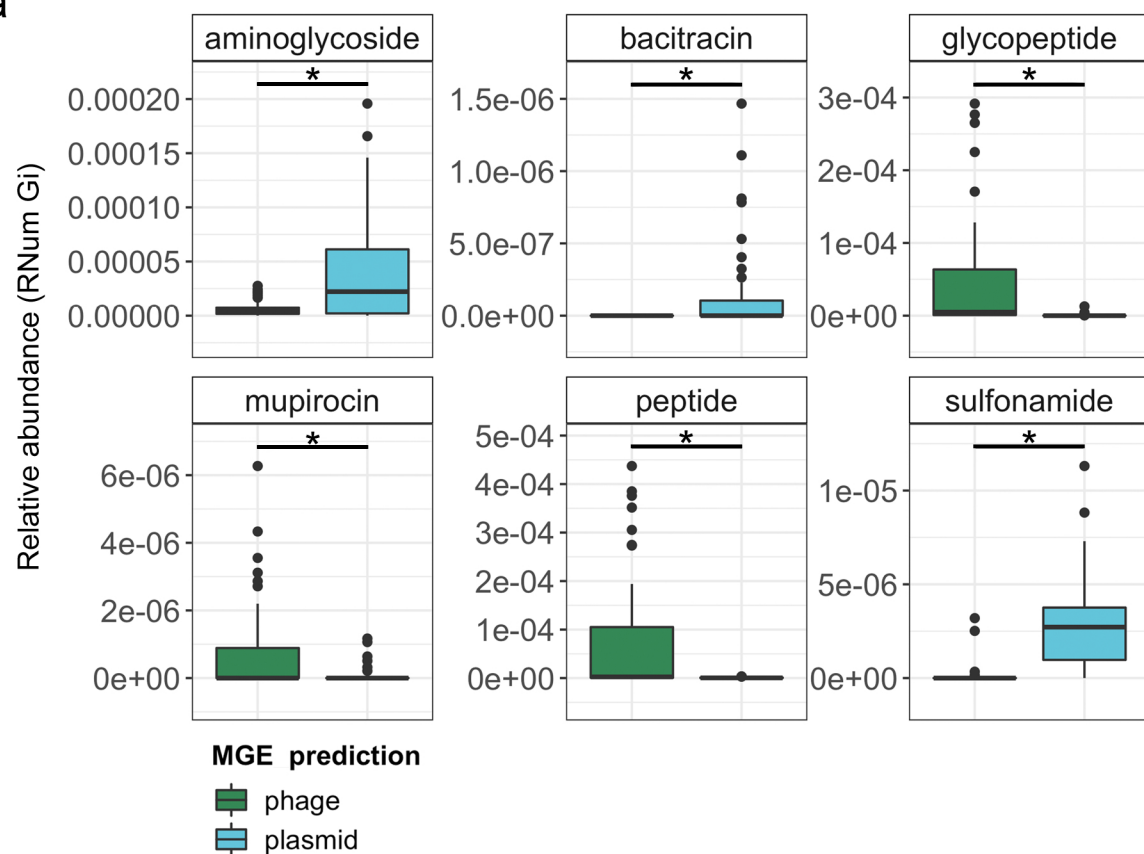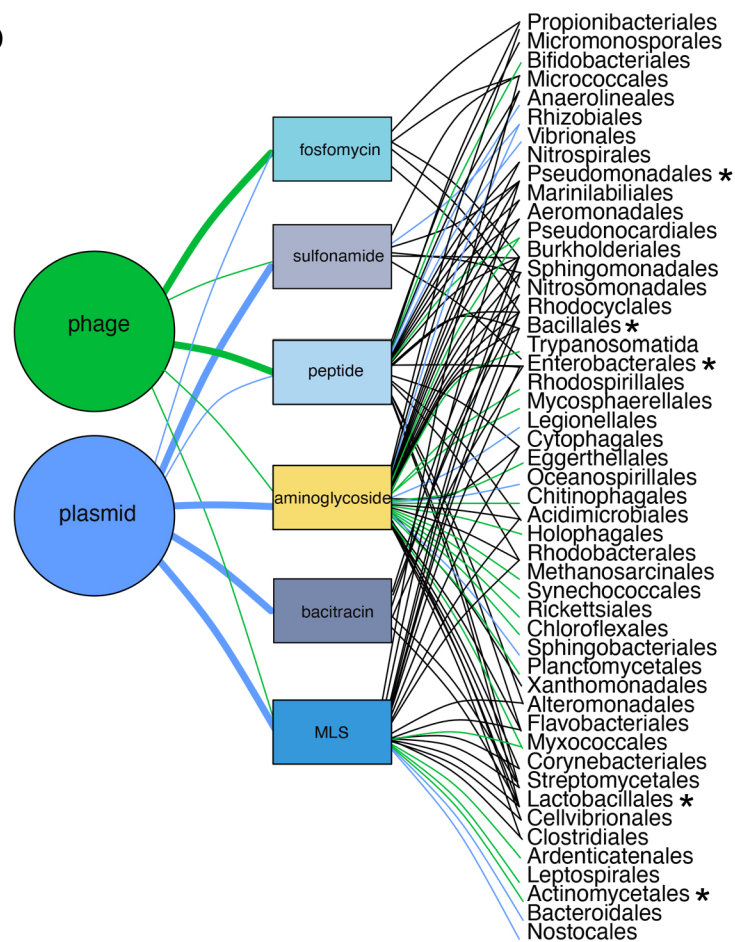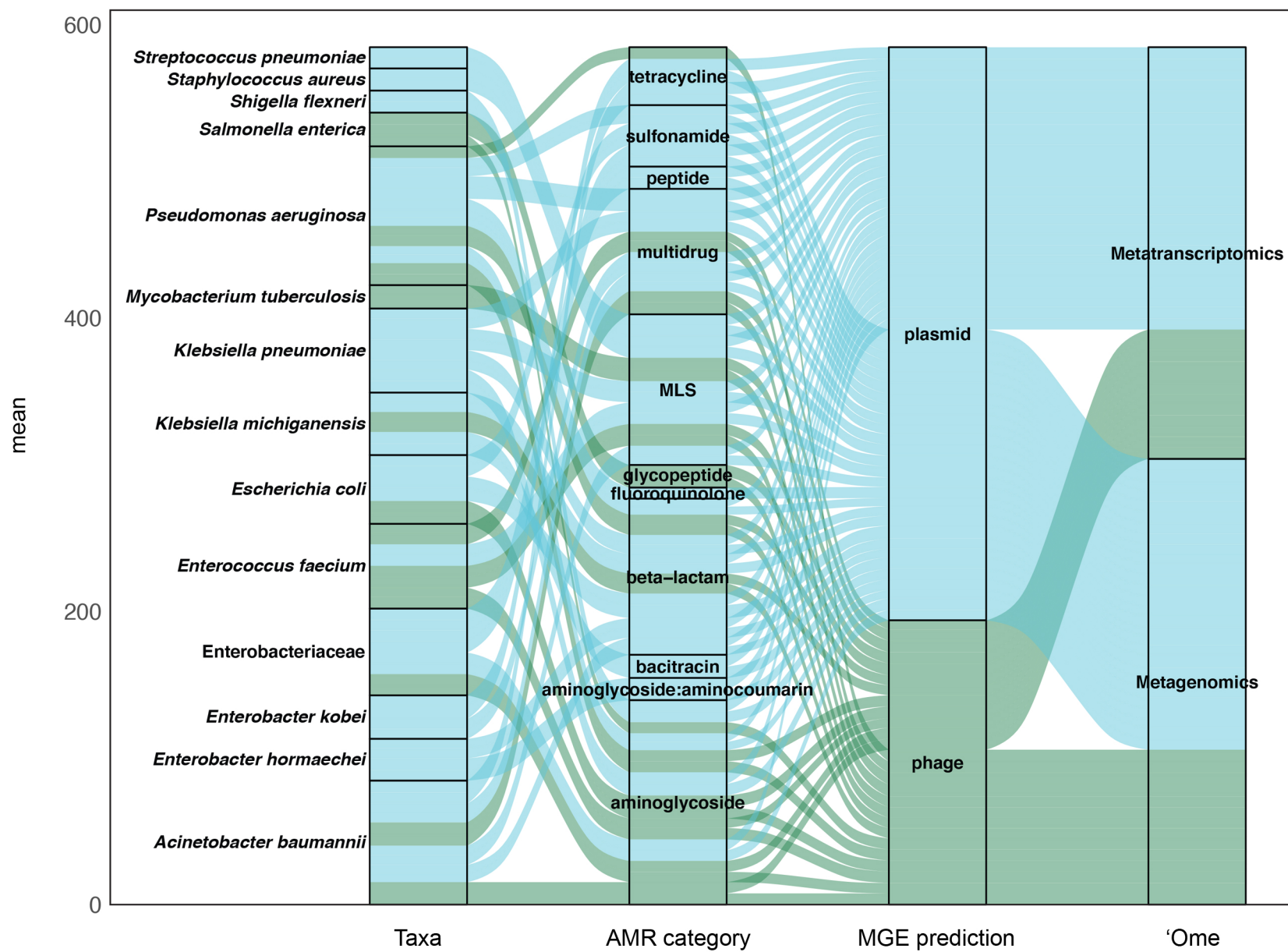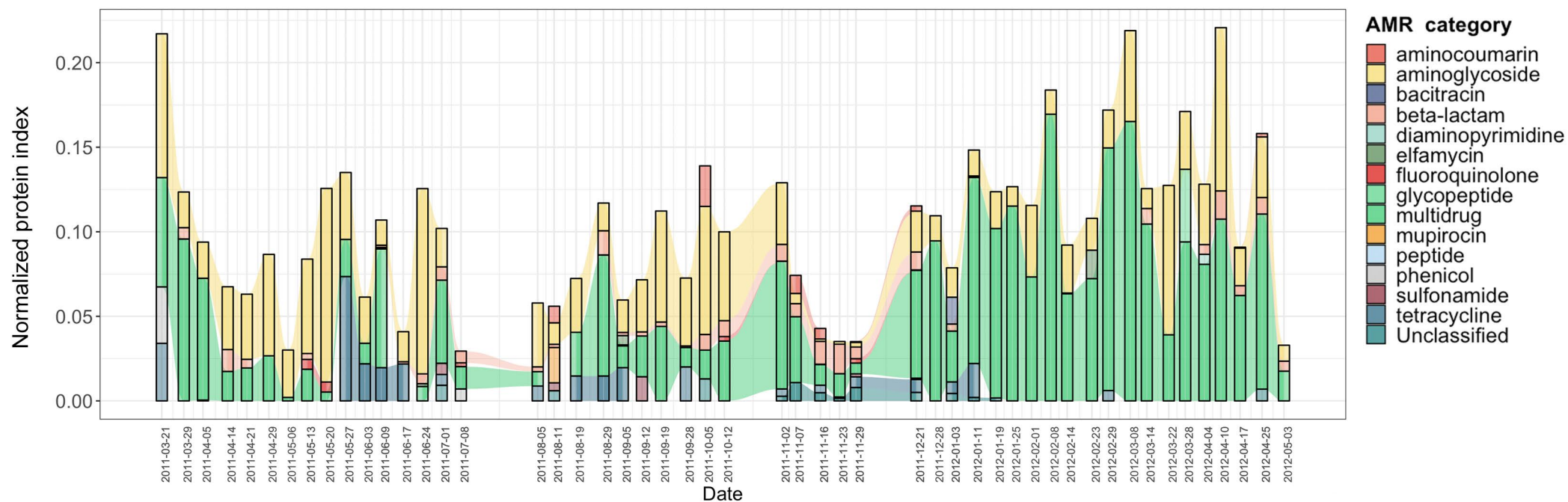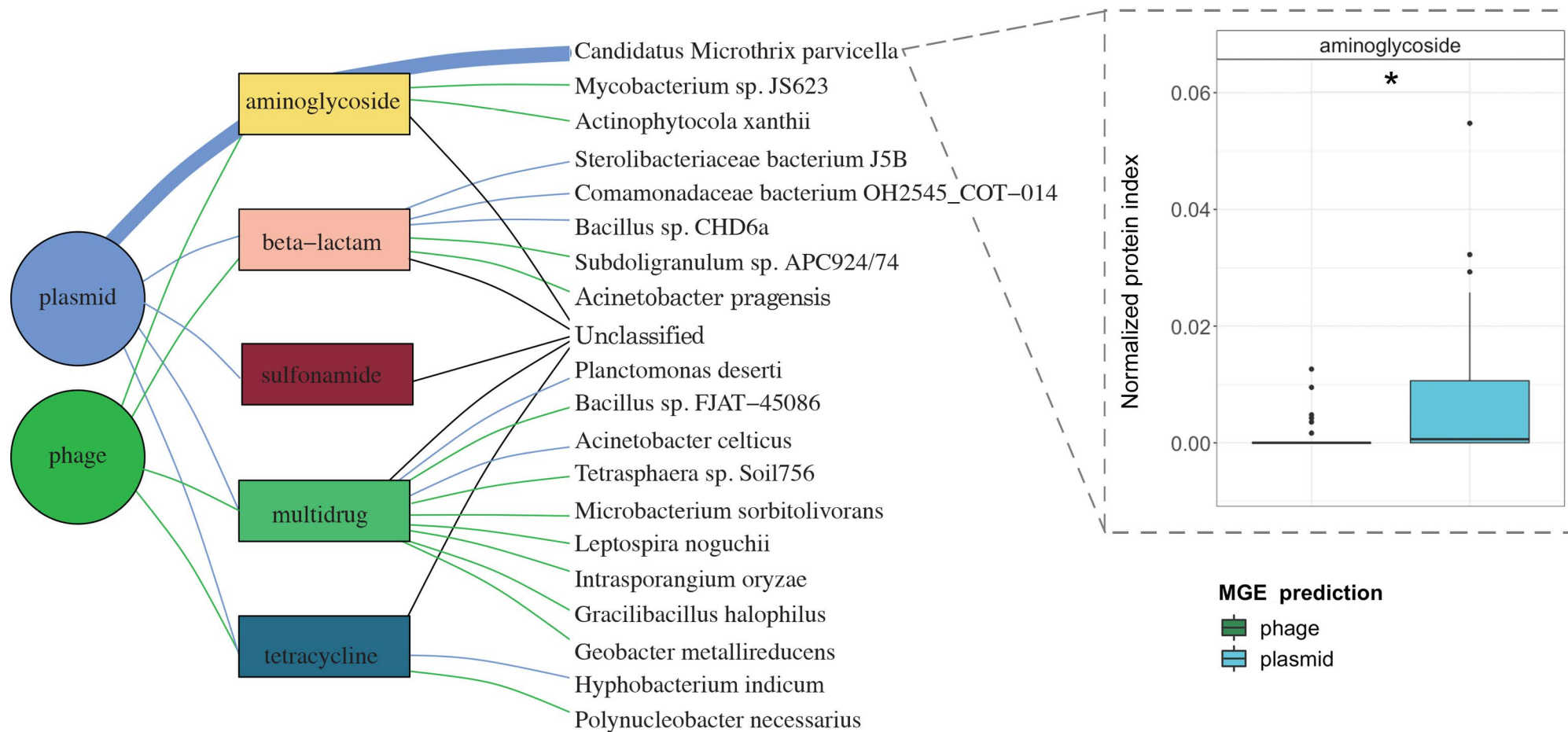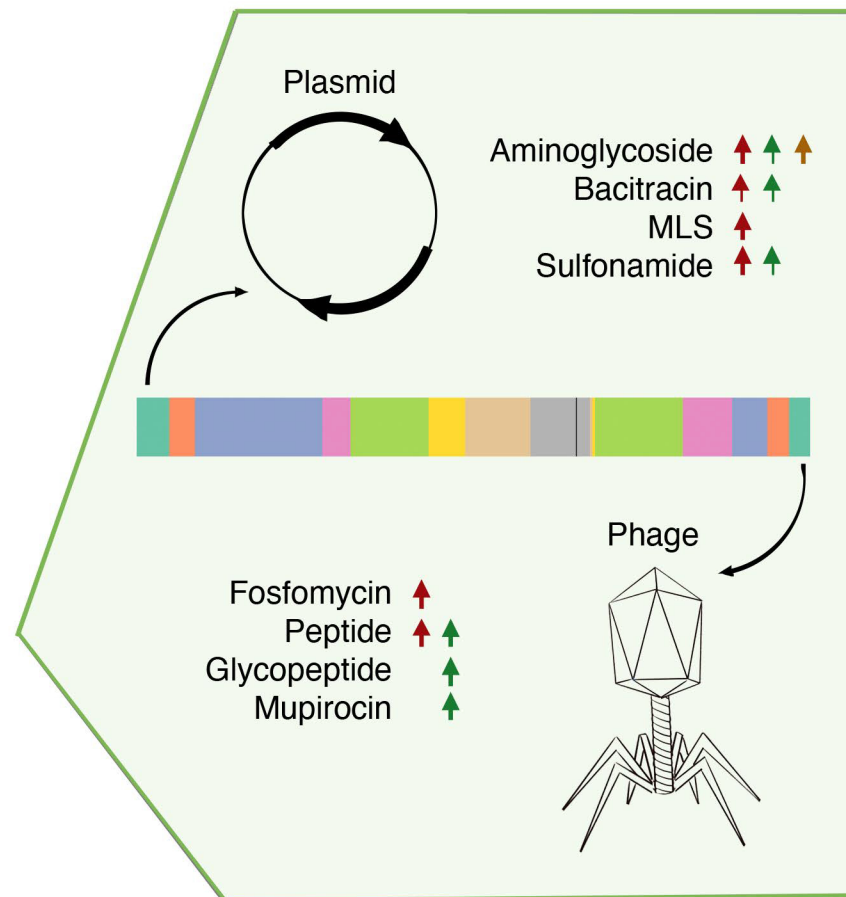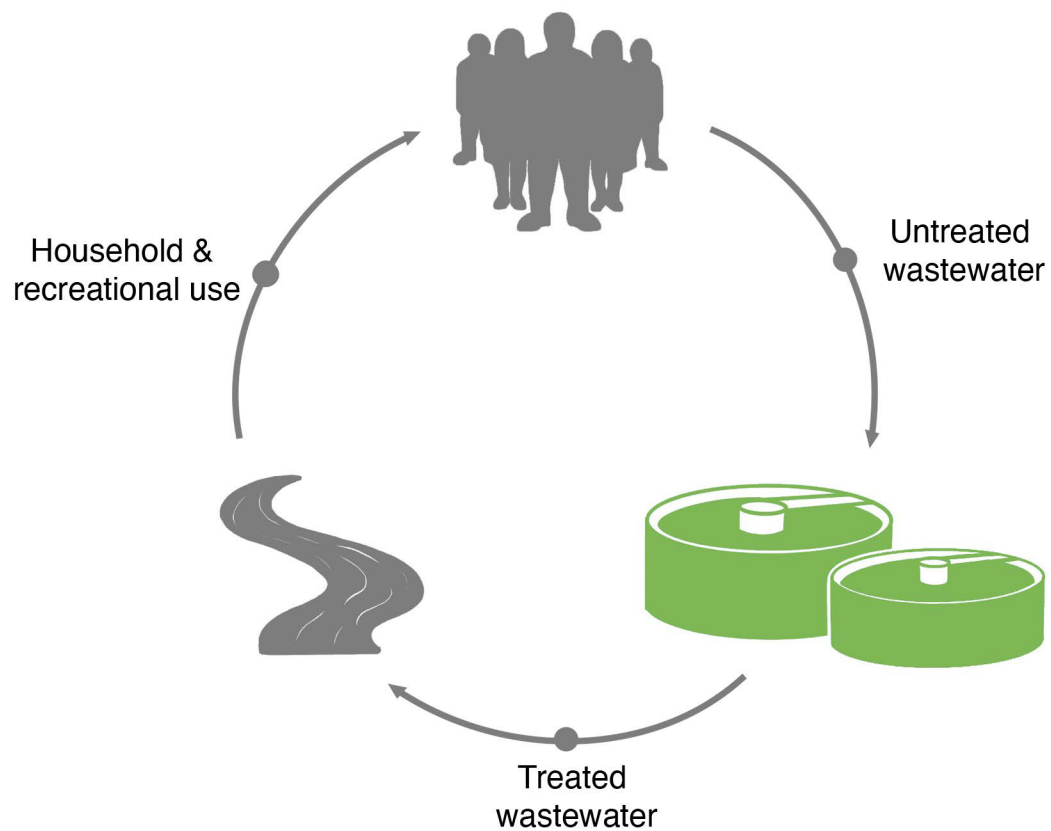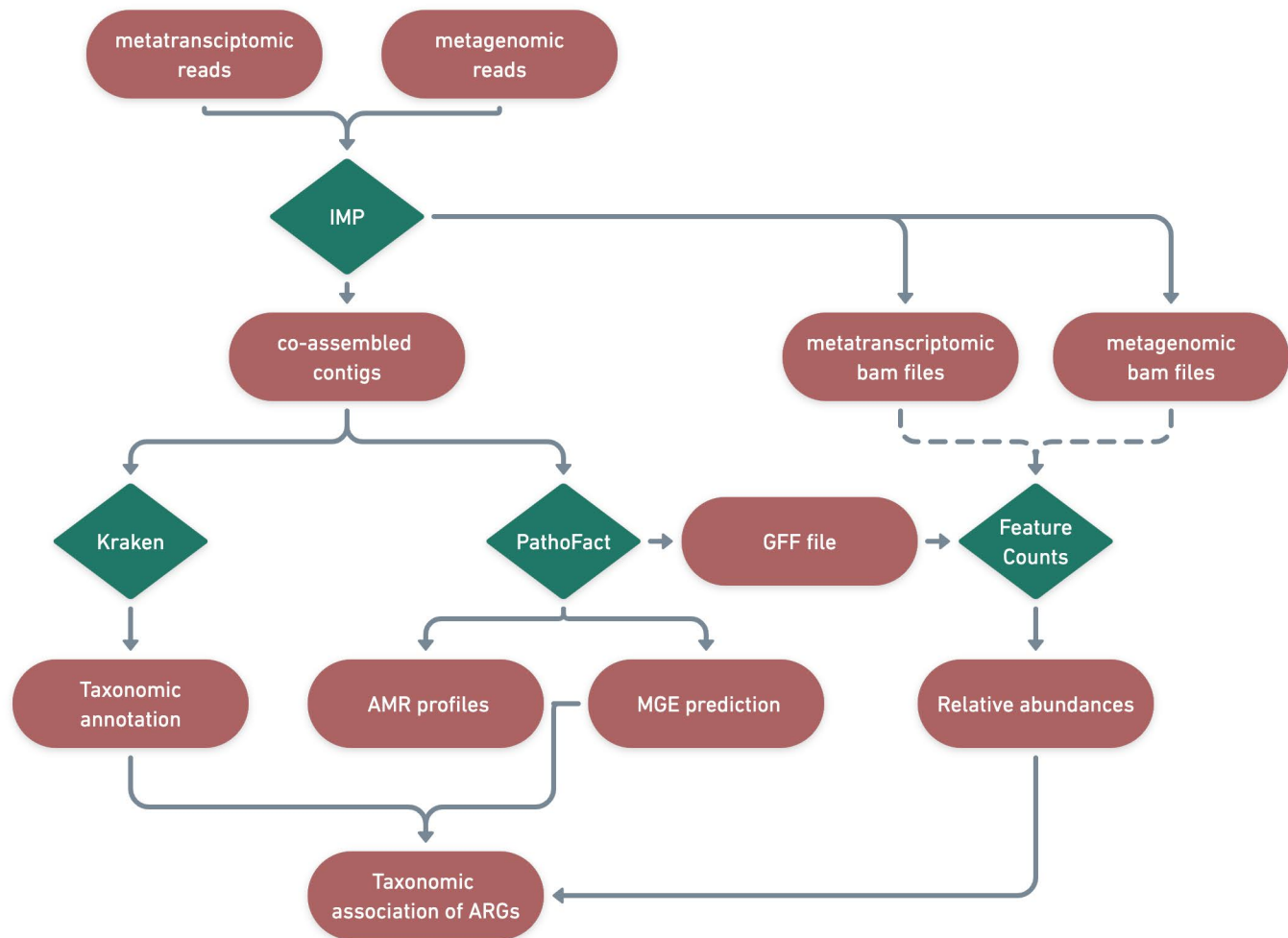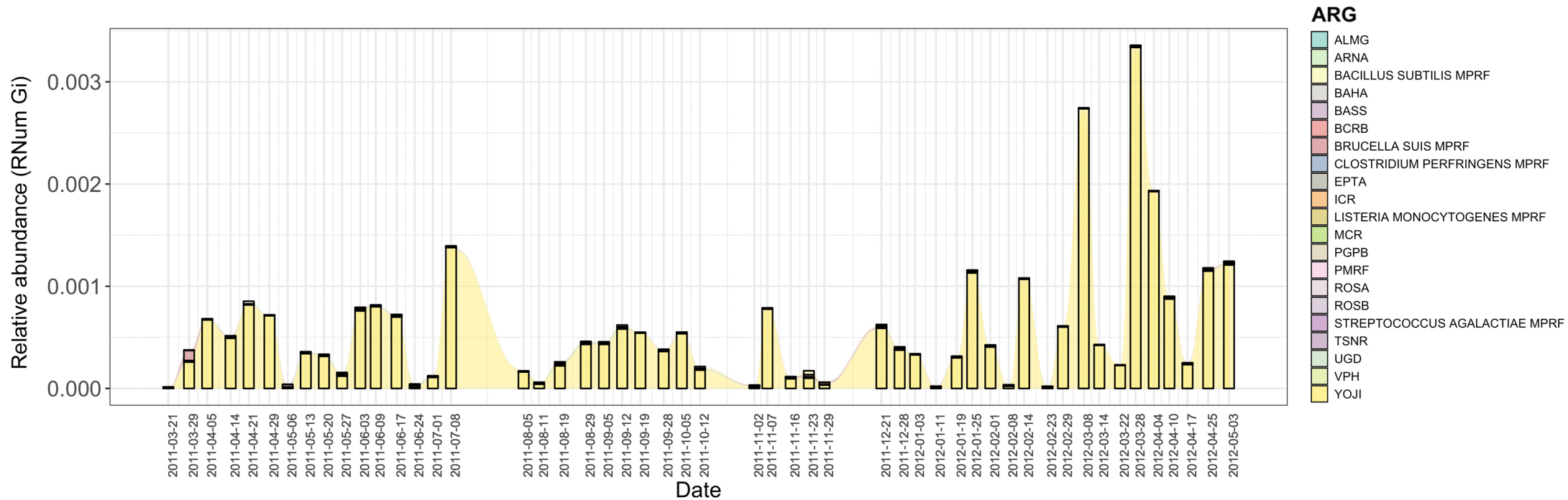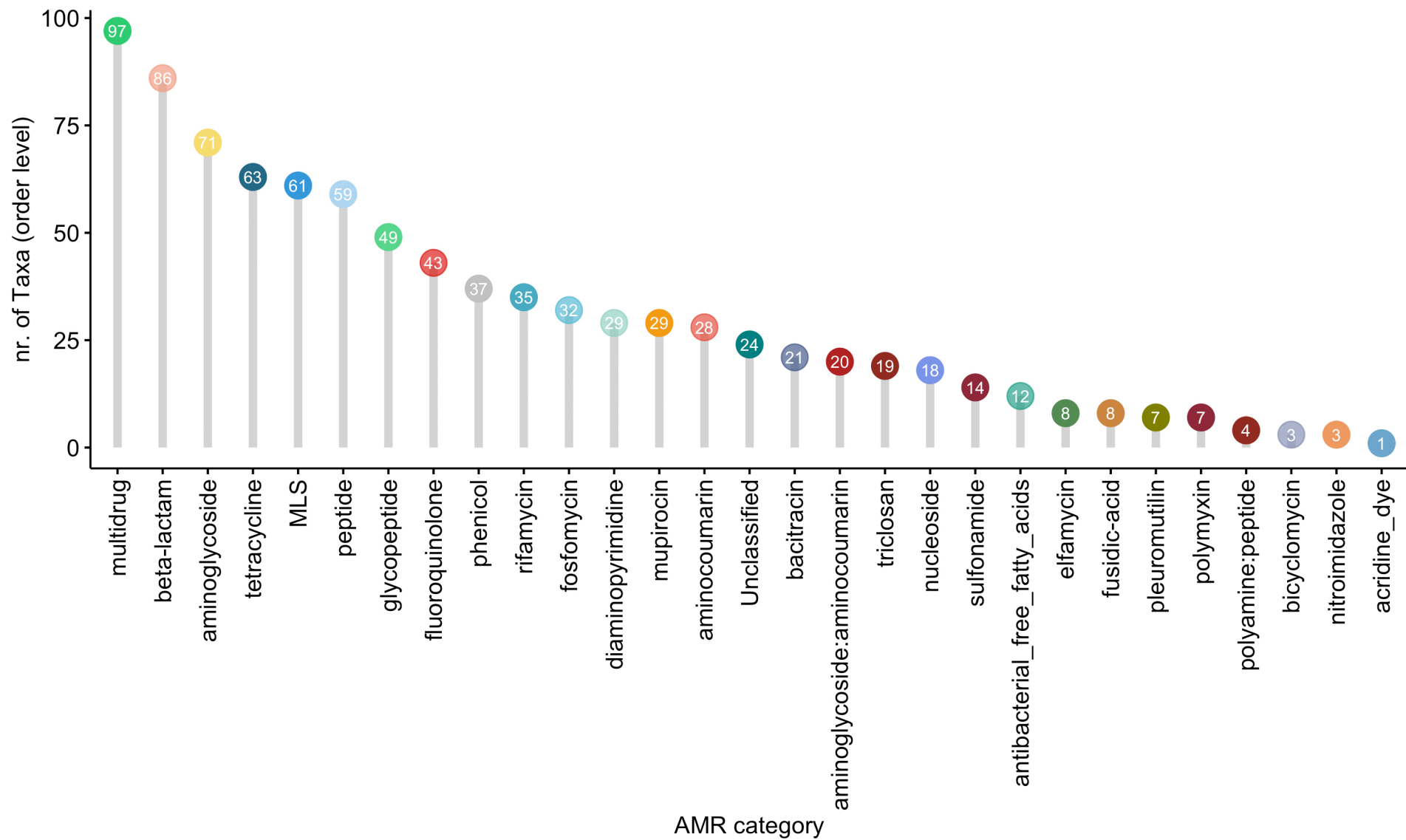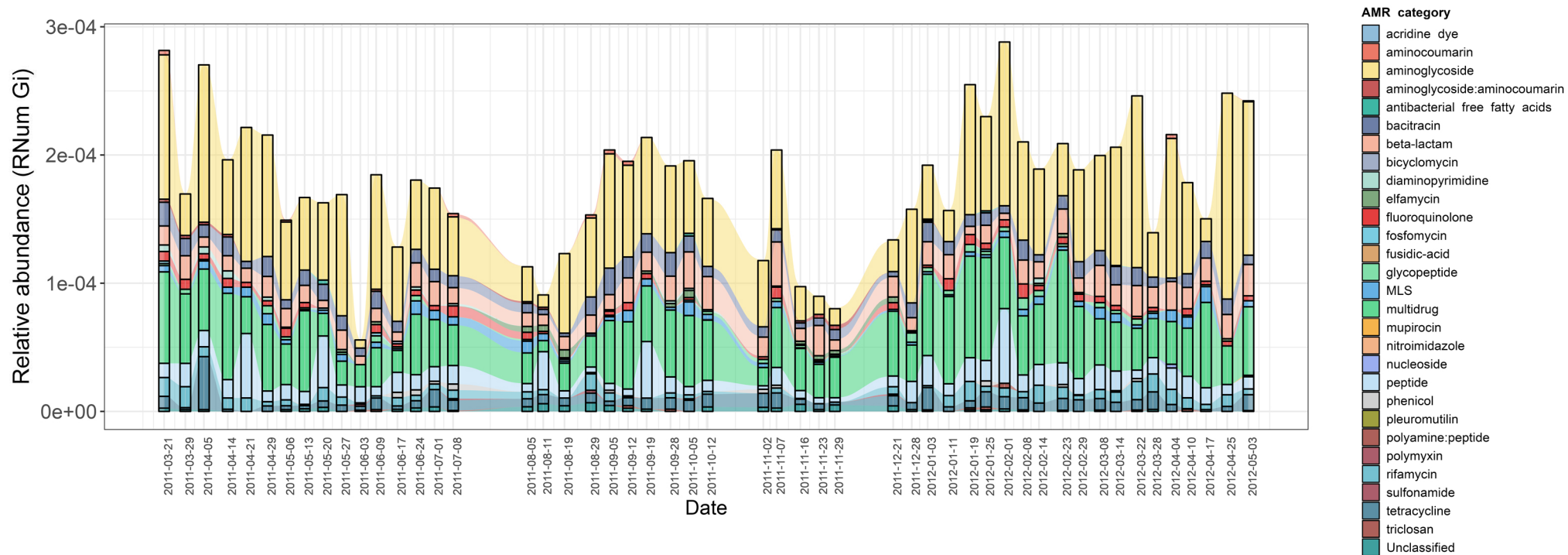
Niche size
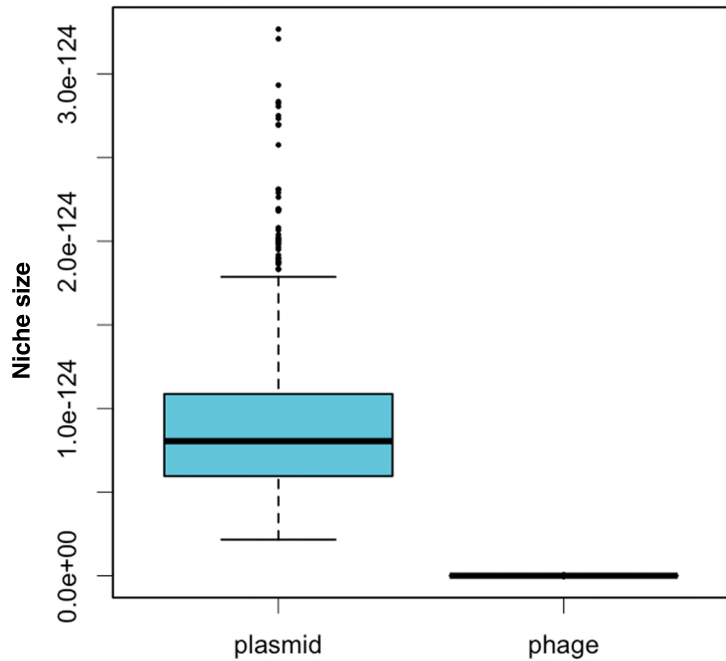
Niche plot: aminoglycoside

a

b

c

d
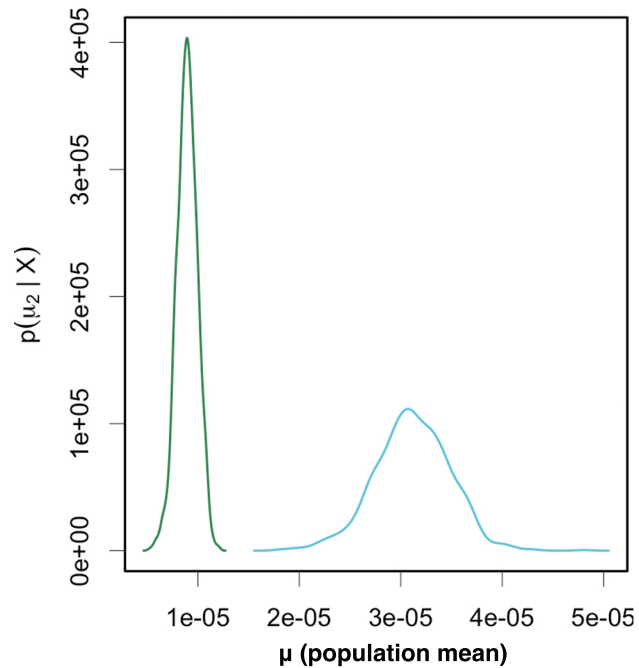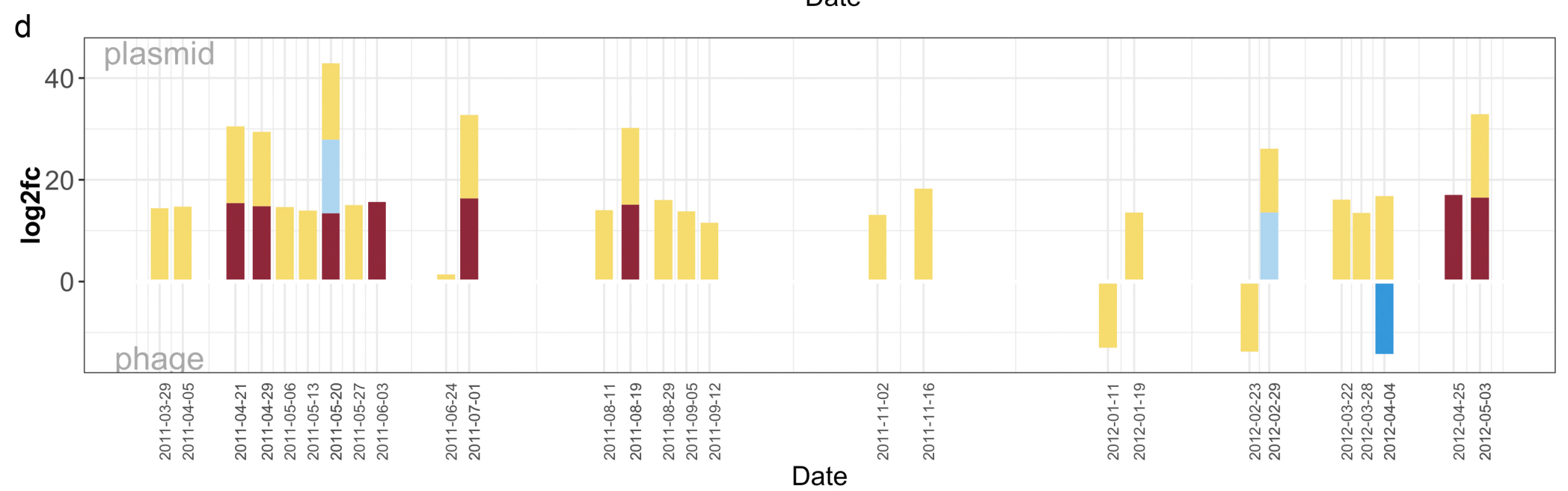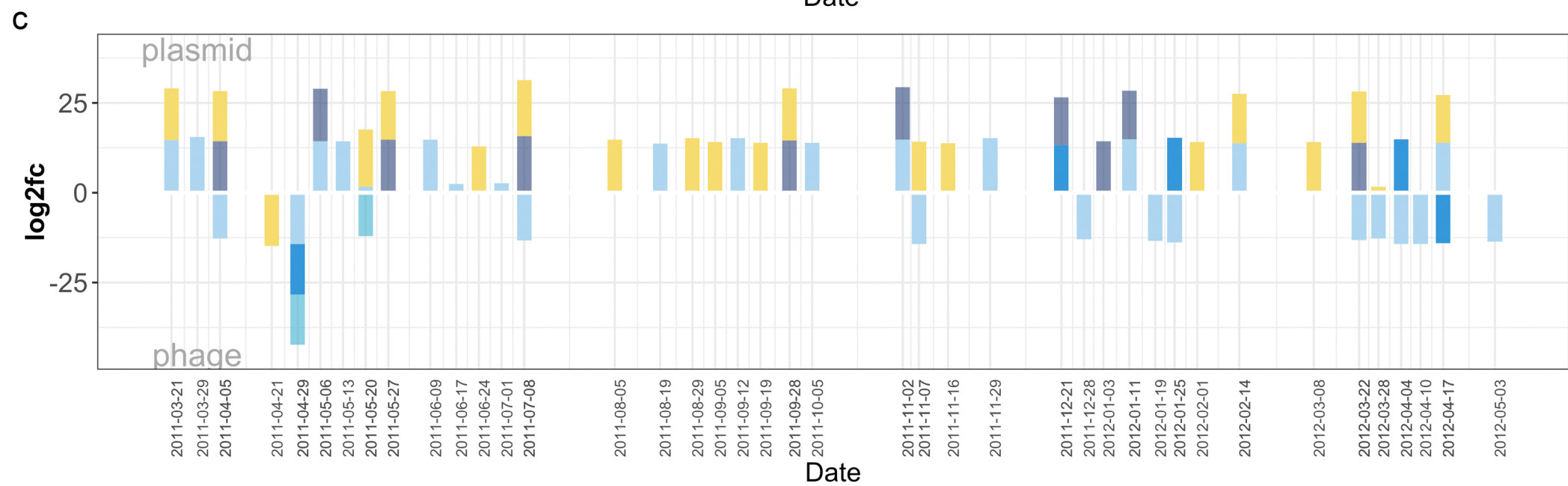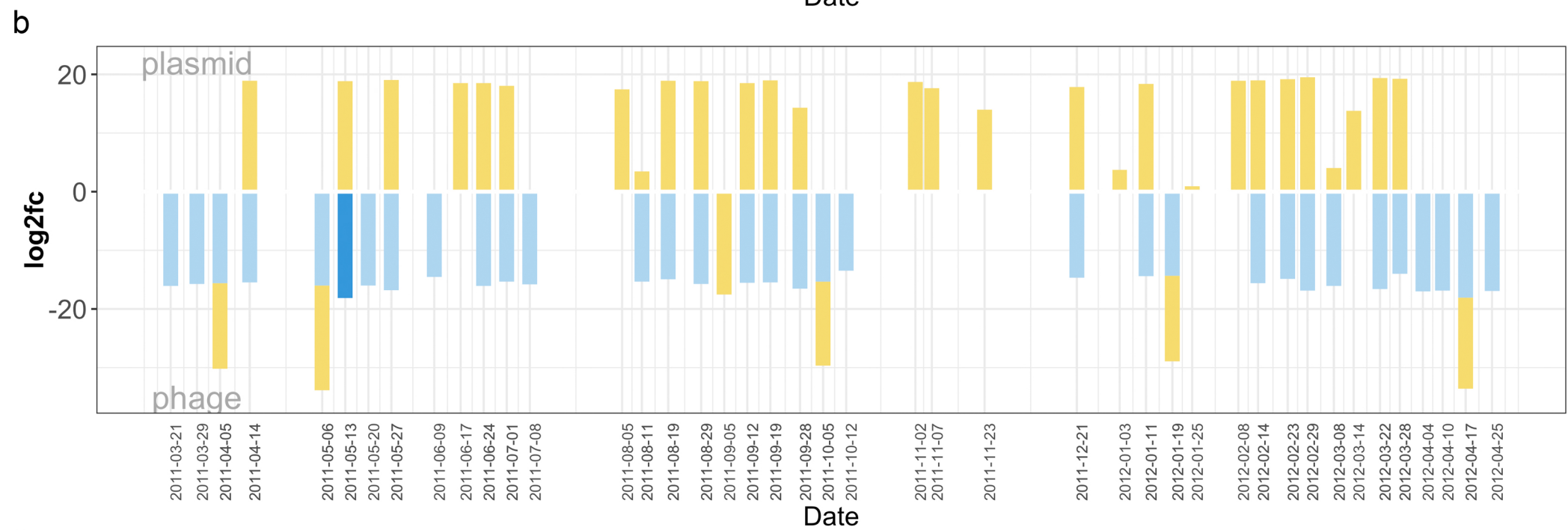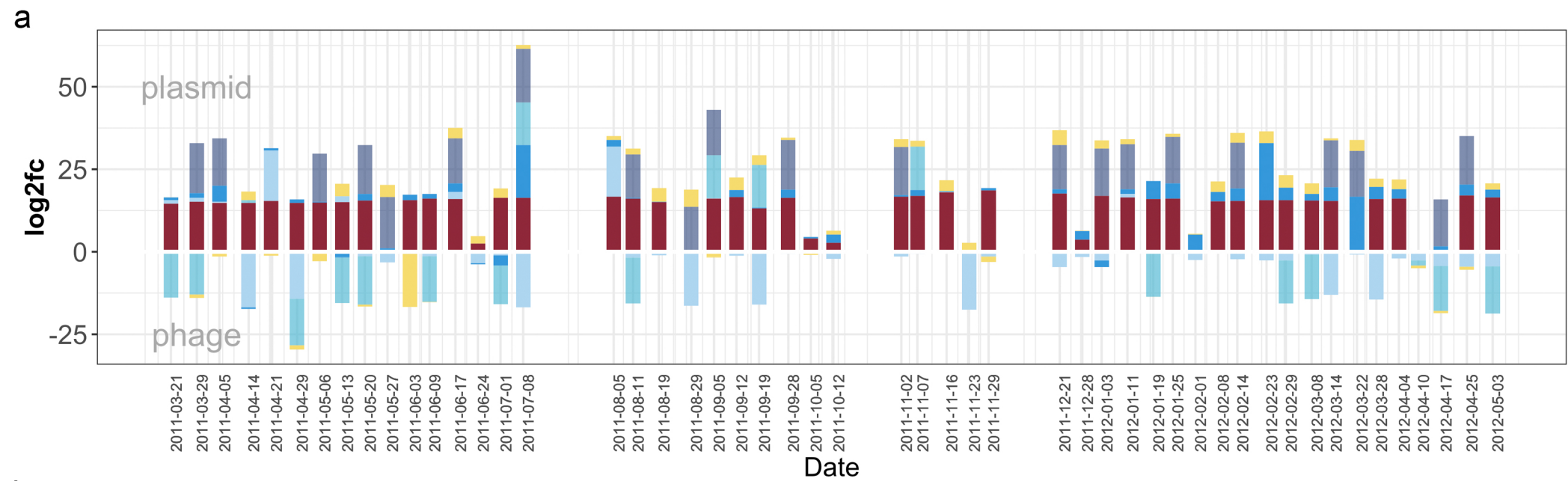
AMR_category

- aminoglycoside
- bacitracin
- fosfomycin
- MLS
- peptide
- sulfonamide

a

b